The Cryosphere Discuss., 5, 2197–2252, 2011
www.the-cryosphere-discuss.net/5/2197/2011/
doi:10.5194/tcd-5-2197-2011

The Cryosphere Discussions

Multi-scale validation of a new soil freezing scheme for a land-surface model with physically-based hydrology

I. Gouttevin[1,2], G. Krinner[1], P. Ciais[3], J. Polcher[4], and C. Legout[5]

[1]Laboratoire de Glaciologie et de Géophysique de l'Environnement (LGGE), UMR5183, CNRS – Université Joseph Fourier – Grenoble 1, 54 rue Molière, BP96, 38402 St Martin d'Hères, France
[2]AgroParisTech, ENGREF, 19 av. du Maine, 75015 Paris, France
[3]Laboratoire des Sciences du Climat et de l'Environnement (LSCE), UMR8212, CEA/CNRS/UVSQ – Orme les Merisiers, 91191 Gif-sur-Yvette, France
[4]Laboratoire de Météorologie Dynamique (LMD), UMR8539, CNRS – Ecole Polytechnique/ Ecole Normale Supérieure de Paris/UPMC, 4 place Jussieu, 75252 Paris, France
[5]Laboratoire d'étude des Transferts en Hydrologie et Environnement (LTHE), UMR5564, CNRS/G-INP/IRD – Université Joseph Fourier – Grenoble 1, 70 rue de la Physique, 38400 St Martin d'Hères, France

Received: 6 July 2011 – Accepted: 7 August 2011 – Published: 23 August 2011

Correspondence to: I. Gouttevin (gouttevin@lgge.obs.ujf-grenoble.fr)

Published by Copernicus Publications on behalf of the European Geosciences Union.

Abstract

Soil freezing is a major feature of boreal regions with substantial impact on climate. The present paper describes the implementation of the thermal and hydrological effects of soil freezing in the land surface model ORCHIDEE, which includes a physical description of continental hydrology. The new soil freezing scheme is evaluated against analytical solutions and in-situ observations at a variety of scales in order to test its numerical robustness, explore its sensitivity to parameterization choices and confront its performances to field measurements at typical application scales.

It is shown that the appropriate vertical discretization to represent the thermal freezing dynamics is centimetric, and the appropriate freezing window is 1 to 2 °C wide. Furthermore, linear and thermodynamical parameterizations of the liquid water content lead to similar results in terms of water redistribution within the soil as a consequence of freezing.

The new soil freezing scheme considerably improves the representation of runoff and river discharge in regions underlain by permafrost and subject to seasonal freezing. A thermodynamical parameterization of the liquid water content appears more appropriate for an integrated description of the hydrological processes at the scale of the vast Siberian basins. The use of a subgrid variability approach and the representation of wetlands could help capturing the features of the Arctic hydrological regime with more accuracy.

The modelling of the soil thermal regime is generally improved by the representation of soil freezing processes. In particular, the dynamics of the active layer is captured with an increased accuracy by the soil freezing module, which is of crucial importance in the prospect of simulations involving the response of frozen carbon stocks to future warming. A realistic simulation of the snow cover and its thermal properties, as well as the representation of an organic horizon with specific thermal characteristics, are confirmed to be a pre-requisite for an accurate modelling of the soil thermal dynamics in the Arctic.

TCD
5, 2197–2252, 2011

1 Introduction

Frozen soils occupy 55 to 60 % of the land surface of the Northern Hemisphere in winter (Zhang et al., 2003) with considerable implications for climate (William and Smith, 1989).

Soil freezing impedes water infiltration and drainage, leading to a modified hydrological regime at catchment's scale (Woo et al., 2000). Arctic rivers provide an example of large scale hydrological implications of soil freezing: the seasonal cycle of freshwater input into the Arctic Ocean is highly modulated by terrestrial freeze-thaw cycles (Barry and Serreze, 2000); this freshwater input is of major importance since it partly controls the Arctic Ocean's salinity, sea-ice formation and finally the global thermohaline circulation (McDonald et al., 1999; Peterson et al., 2002; Aagaard and Carmack, 1989; Arnell 2005). In Eurasia, Serreze et al. (2002) found that the runoff to precipitation ratio was proportional to the extent of permafrost in each river basin. Generally, watershed underlain with permafrost have a low subsurface water storage capacity (Kane, 1997), implying low winter river discharges and fast hydrological responses.

At smaller scales, freeze-thaw cycles induce lateral and vertical water redistribution as a consequence of cryosuction, patterned ground, talik or thermokarst lakes formation. Those features modify the soil structure, its water holding capacity, moisture content, and the water available for plants and for the soil biota, with potential consequences on water fluxes between the soil and the atmosphere, vegetation growth and the carbon dynamics within the soil (Pitman et al., 1999).

Another consequence of soil freezing is the latent heat release and consumption, which delay the seasonal soil temperature signal (Boike et al., 1988). Frozen soils also exhibit specific thermal characteristics due to the differences of thermal conductivity and heat capacities between ice and water, and dissimilarities in water distribution within the soil column (e.g. Farouki, 1981).

Arctic and boreal regions are in great part underlain by permafrost and/or subject to seasonal freezing. Their soils contain more than 40 % of the global terrestrial carbon

TCD
5, 2197–2252, 2011

(Tarnocai, 2010), undergoing slow or no decomposition due to cold temperatures. The soil microbiological activity is indeed highly sensitive to temperature, especially in subfreezing states (Nobrega et al., 2007); the organic matter decomposition pathway (soil respiration or methanogenesis) also depends on the hydric state of the soil. An accurate representation of soil temperature and moisture content as modulated by soil freezing in boreal regions is all the more crucial as evolutions related to climate change have already been perceived at high latitudes (Serreze et al., 2000) and global climate models project the strongest future warming for those regions (IPCC, 2007), with potential destabilization of their massive carbon pool.

Given the importance of frozen ground to water, energy and carbon cycling, soil freezing stands out as a critical feature for land surface and global climate modelling (Pitmann et al., 1999; Quinton et al., 2005; Yi et al., 2006). Efforts have been recently made to introduce freeze-thaw algorithms in land-surface models (Luo et al., 2003), which now involve a physically-based hydrology (e.g. Slater et al., 1998; Smirnova et al., 2000; Essery et al., 2001; Bonan et al., 2002). However, few of these models are designed to embed or be coupled with a detailed carbon cycle module (Khvorostyanov et al., 2008).

The present paper is dedicated to the description and validation of a numerical, 1-D soil freezing scheme designed to be part of the physically-based hydrological scheme of the land-surface and carbon model ORCHIDEE (Organizing Carbon and Hydrology Into Dynamical EcosystEms, Krinner et al., 2005). ORCHIDEE commonly provides surface boundary conditions to the atmospheric model LMDZ, but is also used off-line for a variety of applications at scales ranging from point location to global, hence the need for a multi-scale validation approach. Special attention is given to parameterization and numerical choices and their limits in the context of the current representation of soil freezing in land surface models.

The first part fully describes the soil freezing scheme within the model's framework. In a second part, the accuracy of the scheme is verified against semi-analytical and empirical solutions; its sensitivity to parameterization choices is discussed. Finally, simulation results at different scales are compared with field data, which helps diagnosing the improvements induced by the freezing scheme and defining further development prospects.

2 The soil freezing scheme

2.1 Soil hydrological and thermal processes in the land-surface model ORCHIDEE

ORCHIDEE is the land surface model part of the fully coupled climate model IPSL-CM4 but can be run off-line, driven by a prescribed atmospheric forcing (e.g. reanalyses or outputs from an atmosphere model). It combines a soil vegetation atmosphere transfer model with a carbon cycle module computing a vertically detailed carbon dynamics. Although the implications of soil freezing on the carbon cycle are beyond the scope of this paper, the vertically discretized hydrological and carbon modules of ORCHIDEE should provide a useful tool for investigating these interactions.

ORCHIDEE computes all the soil-atmosphere-vegetation relevant energy and water exchange processes at 30-min time steps. It is made out of different routines respectively dedicated to energy balance, interaction with the canopy, soil temperatures, soil moisture content, and routing of water towards the oceans. Extended model description can be found in Krinner et al. (2005), de Rosnay (1999) and d'Orgeval et al. (2008) for the vertically discretized hydrology. We hereafter only detail the soil hydrological and thermal parameterizations of the model, which are affected by soil freezing.

ORCHIDEE allows to choose between a simple hydrological scheme based on 2 reservoirs following the work of Choisnel (1977), and a vertically discretized hydrological scheme computing vertical water fluxes at each time step (de Rosnay, 1999; d'Orgeval, 2008). Lateral water fluxes are only allowed from one grid-cell to another and do not affect the soil water content, as explained later in the description of the routing scheme. A parameterization of soil freezing exists in the simple hydrology (Koven et al., 2009; Ringeval et al., 2011); however, the improvements induced by a vertically discretized hydrology on the modelling of land-atmosphere water and energy fluxes (de Rosnay, 1999) advocate for the use of a physically-based hydrology and subsequent implementation of soil freezing parameterizations.

ORCHIDEE vertically discretized hydrology derives from the model of the Centre for Water Resources Research (Dooge et al., 1997). It computes the water balance at different depths within the soil profile. Only vertical water movements induced by gravity and suction are accounted for, while water vapour diffusion and water migration driven by osmotic or thermal gradients are ignored. The evolution of soil moisture is thus represented by the 1-D Richards' equation:

$$\frac{\partial \theta}{\partial t} = \frac{\partial}{\partial z}\left(K(\theta)\cdot\left(\frac{\partial \Psi(\theta)}{\partial z} - 1\right)\right) - S \tag{1}$$

with Ψ: water suction e.g. absolute value of matric potential (m), θ: volumetric water content ($\mathrm{m\,m^{-1}}$), z: depth axis, pointing towards the surface, K: hydraulic conductivity ($\mathrm{m\,s^{-1}}$), S: sink term corresponding to water uptake by roots ($\mathrm{s^{-1}}$).

Equation (1) is discretized on 11 numerical nodes distributed within the soil, with a finer resolution near the surface where key hydrological processes (infiltration, evaporation) take place. The uppermost layer is 2 mm thick and the thickness of the layers increases as a geometric sequence of ratio 2 with increasing depth, leading to a total default depth of 2 m for hydrological processes. The numerical scheme relies on implicit finite differences and is unconditionally stable. Bottom boundary condition is gravity drainage. At the top of the soil column, the water flux towards the soil is set to infiltration minus evaporation and modulated by the infiltration capacity and water content of the soil.

Matric potential and hydraulic conductivity formulations rely on a Van Genuchten (1980)-Mualem (1976) parameterization:

$$\Psi(\theta) = \frac{1}{\alpha}\left[\left(\frac{\theta - \theta_r}{\theta_s - \theta_r}\right)^{-\frac{1}{m}} - 1\right]^{\frac{1}{n}} \tag{2}$$

TCD
5, 2197–2252, 2011
Multi-scale validation of a new soil freezing scheme
I. Gouttevin et al.

$$K(\theta) = K_s \left(\frac{\theta-\theta_r}{\theta_s-\theta_r}\right)^l \left[1-\left(1-\left(\frac{\theta-\theta_r}{\theta_s-\theta_r}\right)^{\frac{1}{m}}\right)^m\right]^2 \quad (3)$$

with θ_s: saturated water content ($m^3\,m^{-3}$), θ_r: residual water content ($m^3\,m^{-3}$), α: Van Genuchten parameter (m^{-1}), related to the inverse of the air entry suction, m and n: Van Genuchten parameters related to pore-size distribution ($m = 1 - \frac{1}{n}$ according to the Mualem model), l: Van Genuchten parameter related to tortuosity ($l = 0.5$ in the Mualem model), K_s: saturated hydraulic conductivity ($m\,s^{-1}$).

The parameters α, m, n, and K_s are soil-type dependent. Saturated hydraulic conductivity typically varies over several orders of magnitude from coarse to fine-textured soils (Fig. 1a), with considerable impact on the soil water regime. Three different soil types (coarse, medium and fine) associated with specific hydraulic parameters are accounted for in ORCHIDEE (Table 1). The soil types repartition is the result of the original Food and Agriculture Organization map (1978) and interpolation work by Zobler (1986). In ORCHIDEE, the original 5 textural classes used by Zobler (fine, medium-fine, medium, medium-coarse, and coarse) are reduced to 3 textural classes (fine, medium, coarse) with the medium class composed out of the medium fine, medium and medium coarse FAO classes. The hydraulic characteristics of the three ORCHIDEE soil textural classes originate from Carsel and Parrish (1988) for the referent USDA (1994) name (Table 1).

Overland flow and drainage water are routed towards the outflow of the major rivers via a routing module thoroughly described in NgoDuc et al. (2007). Basically, the overland flow is transferred to a "fast" reservoir while drainage fuels a "slow" reservoir. Both reservoirs eventually flow into the downstream grid-cell "stream" reservoir, which represents the rivers. The drainage transfer rate from the upstream "slow" reservoir to the downstream "stream" reservoir is slower than the overland flow transfer rate from the upstream "fast" to the downstream "stream" reservoir. The "stream" reservoir water is eventually routed from one grid-cell to another till the mouth of the river is reached.

All transfer and routing rates depend on the river length from the upstream grid-cell to the down-stream grid-cell and the height loss over that path.

The soil temperature is computed according to the Fourier equation using a finite difference implicit scheme with usually 7 thermal nodes geometrically distributed between 0 and 5 m. (Hourdin, 1992). The thermal soil is thus thicker than its hydrological counterpart, a necessary feature when considering that the typical damping depth of the temperature annual cycle is about 3 m (Alexeev et al., 2007). This resolution was shown to be adapted to the representation of diurnal, annual, and decadal temperature signals (Hourdin, 1992). The first thermal layer is 4.3 cm thick and the thickness of each layer is multiplied by 2 as the layers get deeper. The upper boundary condition is the flux equilibrium at the soil surface; the lower boundary condition is a zero thermal flux. Latent heat sources and sinks within the soil are by default not included; thermal advection through water movements is neglected. Soil thermal properties depend on the water content, which is interpolated each 30 min time-step from the hydrological module at the 7 thermal nodes.

2.2 The new soil freezing scheme

The new soil freezing scheme described below aims at accounting for latent heat effects within the soil and for soil-freezing induced changes in the thermal and hydrological properties of the ground. Current numerical soil freezing algorithms implemented in land surface models differ in their representation of those effects. The new parameterizations introduced in ORCHIDEE are hereafter detailed and compared with their concurrent counterparts.

Latent heat is a source or a sink term in the Fourier equation. With the assumptions of no thermal advection and no phase change implying the gas phase, the 1-D Fourier equation with latent heat term writes:

TCD
5, 2197–2252, 2011

$$C_p \frac{\partial T}{\partial t} = \frac{\partial}{\partial z}\left(K_{th} \cdot \frac{\partial T}{\partial z}\right) + \rho_{ice} \cdot L \cdot \frac{\partial \theta_{ice}}{\partial t} \tag{4}$$

with C_p: volumetric soil heat capacity ($\mathrm{J\,K^{-1}\,m^{-3}}$), T: soil temperature (K), K_{th}: thermal conductivity ($\mathrm{W\,m^{-1}\,K^{-1}}$), ρ_{ice}: ice density ($\mathrm{kg\,m^{-3}}$), L: latent heat of fusion ($\mathrm{J\,kg^{-1}}$), θ_{ice}: volumetric ice content ($\mathrm{m^3\,m^{-3}}$).

During freeze-up, latent heat release will delay the freezing front progression. Conversely, latent heat consumption will counteract warming as subfreezing temperature reaches the freezing point. As it systematically opposes the temperature change, latent heat adds up to inertia, which is the basis of its incorporation into an apparent heat capacity in models (Fuchs, 1978). This ploy allows to numerically compute a simple diffusion scheme with no source term (Poutou et al., 2004) and is illustrated by the rewriting of Eq. (4) into Eq. (5):

$$\left(C_p - \rho_{ice} \cdot L \cdot \frac{d\theta_{ice}}{dT}\right) \frac{\partial T}{\partial t} = \frac{\partial}{\partial z}\left(K_{th} \cdot \frac{\partial T}{\partial z}\right) \tag{5}$$

with $\frac{d\theta_{ice}}{dT} \prec 0$.

The apparent heat capacity can then be analytically derived from the parameterization of the soil volumetric ice content as a function of temperature (Cox et al., 1999; Smirnova et al, 2000). However, numerical complications occur due to the singularity at $T = 0\,^{\circ}\mathrm{C}$. We elude this difficulty following the work of Poutou et al. (2004), with a phase change linearly spread over a $2\,^{\circ}\mathrm{C}$ temperature interval between $0\,^{\circ}\mathrm{C}$ and $-2\,^{\circ}\mathrm{C}$. This temperature interval will hereafter be referred to as the freezing window ΔT. The model sensitivity to the width of the freezing window will be analyzed in Sect. 3. The apparent heat capacity thus simply writes:

$$C_{app} = C_p - \rho_{ice} \cdot L \cdot \frac{\Delta\theta_{ice}}{\Delta T} \tag{6}$$

TCD
5, 2197–2252, 2011

where $\Delta\theta_{ice}$ equals the total water content of the layer since all available water is considered to freeze in the freezing window.

For energy conservation reasons, the total water content used by the thermal scheme does not evolve from the freezing onset till the end of the thawing. As soon as a layer is entirely thawed, a temperature correction is applied if the amount of latent energy involved in the thawing of this layer and its preceding freezing do not balance each other as a result of numerical approximations.

Thermal diffusion is governed by heat capacity and conductivity. Heat capacity is little affected by soil freezing since ice and liquid water heat capacities have the same order of magnitude. Conversely, heat conductivity is strongly increased upon freezing since ice is almost four times as conductive as liquid water.

Following Johansen (1975) as advertised by Farouki (1981), heat conductivity K_{th} is calculated as a function of soil water and ice content:

$$K_{th} = (k_{sat} - k_{dry}) \cdot S + k_{dry} \tag{7}$$

with k_{sat}: heat conductivity of ice and/or water saturated soil ($W\,m^{-1}\,K^{-1}$), k_{dry}: heat conductivity of dry soil ($W\,m^{-1}\,K^{-1}$), S: soil total (frozen and unfrozen) saturation degree ($m^3\,m^{-3}$).

The saturated soil conductivity is calculated as:

$$k_{sat} = k_s^{1-\theta_s} \cdot k_i^{(1-f_l)\cdot\theta_s} k_w^{f_l\theta_s} \tag{8}$$

with k_s, k_i and k_w: respective heat conductivities for solid soil, ice and water, f_l: fraction of the liquid soil water, assumed to vary linearly from 1 to 0 between 0 °C and –2 °C, in the “freezing window”.

This parameterization is commonly used in land-surface models (e.g. Verseghy, 1991; Cherkauer and Lettenmeier, 1999) concurrently with the De Vries’ parameterization (De Vries, 1963).

TCD
5, 2197–2252, 2011

The soil heat capacity C_p is computed as the sum of the heat capacities of mineral soil and water:

$$C_p = (C_{\mathrm{iw}} - C_{\mathrm{dry}}) \cdot S + C_{\mathrm{dry}}$$

with $C_{\mathrm{iw}} = f_{\mathrm{l}} \cdot C_{\mathrm{wet}} + (1 - f_{\mathrm{l}}) \cdot C_{\mathrm{icy}}$ the heat capacity of a saturated soil ($\mathrm{J\,m^{-3}\,K^{-1}}$), C_{dry} the dry soil heat capacity ($\mathrm{J\,m^{-3}\,K^{-1}}$), C_{wet} the unfrozen saturated soil heat capacity ($\mathrm{J\,m^{-3}\,K^{-1}}$), C_{icy} the frozen saturated soil heat capacity ($\mathrm{J\,m^{-3}\,K^{-1}}$).

The values of these parameters can be found in Table 2 and originate from Pielke (2001).

Finally, recent studies (Alexeev et al., 2007) pointed out that an extension of the soil thermal modelling to depths greater than 30 m was needed to prevent unrealistic heat accumulation in the lowest soil thermal layers over decadal to centennial time scales, driven by the low zero-flux boundary condition. Simulations over such time-scales are precisely a crucial target for a land-surface model including a representation of permafrost and the carbon cycle, as their evolution is expected to provide consequent feedbacks to the ongoing climate change over the next decades. In the new soil freezing scheme, the soil thermal column is therefore deepened to 90 m, while maintaining the geometrical increase of the layer thicknesses: this vertical extension requires the use of 4 additional layers which are detailed Table 3, along with the default thermal and hydrological vertical resolutions.

The main hydrological impacts of soil freezing are a considerable, though not total, reduction in infiltration and water movements (Burt and William, 1976), concurrent with a low water storage capacity in permafrost regions (Kane, 1997). Those features lead to very specific hydrological regimes in regions underlain with permafrost or subject to long seasonal freezing. Most land-surface schemes assume that water movements within a frozen or partially frozen soil occur through unfrozen films and within an unfrozen porosity. These models often prescribe a reduced hydraulic conductivity for frozen soils but still use the Richards' equation to account for water movements. In the SiB and SiB2 model, Sellers et al. (1996b) and Xue et al. (1996) for instance

TCD
5, 2197–2252, 2011

used a linear function to decrease soil hydraulic conductivity at subfreezing temperatures. Lundin (1990) suggested the use of an exponential impedance factor. Other approaches consider that ice becomes part of the soil matrix, which reduces the porosity and the hydraulic conductivity (Kowalczyk et al., 2006). However, this reduction may be too drastic for large scale applications, where water can infiltrate through specific structures like cracks, dead root passages, or where the soil can be locally unfrozen (Koren et al., 1999).

Our new parameterization of frozen soil hydrological processes relies on the two assumptions that (i) only liquid water can move within a frozen or partially frozen soil, and (ii) the hydraulic conductivity in a frozen or partially frozen soil depends only on the liquid water content and the soil properties, with no consideration of a reduced porosity due to the presence of ice. The induced reduction in hydraulic conductivity is thus less severe than in most of the above-cited approaches, which could help representing the ability of water to infiltrate frozen soils at a model grid-cell scale through preferential pathways (Koren et al., 1999). This approach furthermore exploits the already available Van Genuchten parameterization of hydraulic conductivity as a function of water content (Eq. 3 and Fig. 1a). Essery and Cox (2001) similarly model the hydrological properties of the land surface model MOSES at subfreezing temperatures.

We developed two ways of diagnosing the liquid water content at subfreezing temperature. The first one, hereafter referred to as "LINEAR" freezing, assumes a linear increase of the frozen water fraction from 0 to 1 in the "freezing window", i.e. when temperature goes down from 0 to $-2\,^{\circ}$C. The second one, hereafter referred to as "THERMODYNAMICAL" freezing, computes the thermodynamically allowed liquid water content at subfreezing temperatures, based on the balance between the low energy status of adsorbed and capillary liquid water, and the free energy drop induced by phase change (Black and Tice, 1989; Dall'Amico, 2010). With the assumption of an imposed pressure on ice, Fuchs et al. (1978) derived:

$$\Psi(T) = \left| \frac{L \cdot (T - T_{\mathrm{fr}})}{gT} \right| \tag{9}$$

TCD
5, 2197–2252, 2011
Multi-scale validation of a new soil freezing scheme
I. Gouttevin et al.

with $T_{fr} = 273.15$ K: water freezing point, g: standard gravity (m s^{-2}), T: soil temperature (K).

Equation (9) equally means that soil water under suction Ψ will freeze at temperature T; and if the subfreezing temperature T is observed, the liquid water content has adjusted to the suction Ψ.

Liquid water content and soil matric potential are indeed related at subfreezing temperatures, with a relationship similar to what is observed on the course of drying-wetting experiments (Black and Tice, 1989). This suggests that Eq. (2) can be used for frozen or partially frozen soils. A theoretical explanation often advanced (Dall'Amico, 2010) is the replacement of air in the porous media – whose proportion would increase upon drying – by ice when soil freezes. As the stabilizing capillary interactions differ in magnitude between freezing and drying due to a 2.2 times greater surface tension at the air-water than at the ice-water interface, the use of a factor 2.2 in Eq. (2) is sometimes recommended in freezing-thawing applications (Koopmans and Miller, 1966). As capillary interactions are generally involved at lower suctions than adsorptive processes and affect a greater quantity of water, they explain most of the unfrozen water at temperatures just below freezing, when the effects of liquid water are important (Romanovsky and Osterkamp, 2000). The use of the factor 2.2 thus appears relevant, leading to the following equation to describe the thermodynamically allowed liquid water content at subfreezing temperatures as a result of Eqs. (2) and (9):

$$\frac{L \cdot (T - T_{fr})}{gT} = \frac{1}{2.2} \cdot \frac{1}{\alpha} \left[\left(\frac{\theta - \theta_r}{\theta_s - \theta_r} \right)^{-\frac{1}{m}} - 1 \right]^{\frac{1}{n}} \tag{10}$$

The real liquid water content is however limited by the water available within the soil:

$$\theta_l = \mathrm{MIN}(\theta, \theta_{tot}) \tag{11}$$

with θ_l the liquid water content at a subfreezing temperature (m^3 m^{-3}), θ the thermodynamically allowed liquid water content from Eq. (10) (m^3 m^{-3}), θ_{tot} the total water content (m^3 m^{-3}).

TCD
5, 2197–2252, 2011

In both the LINEAR and the THERMODYNAMICAL approaches the residual water content (see Table 1) does not freeze.

Figure 1b and c respectively display the liquid water content diagnosed as a function of temperature by the LINEAR and THERMODYNAMICAL approaches for the three soil types represented in ORCHIDEE. Fine textured soils retain more liquid water at subfreezing temperatures due to high capillary forces. By contrast, in coarser soils, the decrease in liquid soil water content as a function of temperature is steeper. The simulation was performed with an initial volumetric water content of 0.33 for all soil types at 280 K. Figure 1c also illustrates the limitation of liquid water content by available moisture in coarse soils, since the coarse soil gets depleted in water by gravity drainage before freezing occurs.

The thermodynamical approach is commonly used in land surface models with minor variations (Koren et al., 1999; Cox et al., 1999; Smirnova et al., 2000; Cherkauer and Lettenmeier, 2003). Results yield by the linear and the thermodynamical approaches will be compared in Sects. 3 and 4.

Other alternative approaches include power or modified power function:

$$\theta_\mathrm{l} = a(T - T_\mathrm{fr})^b \tag{12}$$

with b a site specific parameter (e.g. Osterkamp and Romanovsky, 1997); or an ice content determined by total water content and energy loss at $T = T_\mathrm{fr}$ (Slater et al., 1998; Takata and Kimoto, 2000; Kowalczyk, 2006). Site specific calibration requirements disqualify the power function approach for land surface modelling purposes at large scales, while the second was discarded as difficult to conciliate with ORCHIDEE's thermal scheme.

3 Validation against analytical solutions and laboratory experiments

In this section the ability of the new soil freezing model at representing the thermal and hydrological processes involved in freeze-thaw cycles is evaluated against idealized

TCD
5, 2197–2252, 2011

data. By "idealized" we mean data where the unknowns usually restricting the power of model validation (uncertainties in the atmospheric forcing, uncertainties in the soil and vegetation parameters, errors or error compensations due to processes not represented by the model) are minimized. The analytical solution of the freezing front progression by Stefan (1890) is one of such datasets for the thermal processes: the model soil thermal parameters and boundary conditions can entirely match their counterpart in the analytical solution, which allows to perform an unbiased model-to-solution comparison and to evaluate the model sensitivity to parameterization or numerical choices. In the absence of any analytical solution for Eq. (1) in frozen or partially frozen conditions, a laboratory monitoring of the liquid water content of a soil column undergoing freezing by Mizoguchi (1990), is used as a benchmark for the hydrological parameterizations.

3.1 Validation of the thermal scheme against the Stefan solution

1-D phase change problems can analytically be solved (Stefan, 1890) with the assumptions of a linear temperature gradient within the soil, a uniform and constant heat conductivity in the frozen zone, and a steady upper boundary condition (Li and Koike, 2003). The solution is obtained from the balance between the latent heat released by the freezing of an infinitesimally thin soil layer, and the heat flux towards the surface integrated over the corresponding infinitesimal time step. The freezing front z progression thus writes as a function of time t, heat conductivity K_{th}, surface temperature difference from the freezing point $T_{\mathrm{s}} - T_{\mathrm{fr}}$, volumetric water content θ, latent heat of fusion L and water density ρ:

$$z = \sqrt{2 \cdot K_{\mathrm{th}} \cdot \frac{(T_{\mathrm{s}} - T_{\mathrm{fr}})}{\theta \cdot L\rho} \cdot t} \tag{13}$$

The freezing front progression simulated by ORCHIDEE is hereafter compared to this analytical solution. To suit the conditions for a comparison, ORCHIDEE is set up in

TCD
5, 2197–2252, 2011

the exact conditions of the Stefan resolution. To have a constant and uniform heat conductivity in the frozen zone, the soil volumetric water content is artificially set at a constant and uniform value. Soil temperature is uniformly initialized at 0 °C, and a step-like temperature surface forcing of −6 °C is applied from $t = 0$ on. The numerical values thus obtained and used for comparison with Eq. (13) are: $K_{th} = 1.05\,\mathrm{W\,m^{-1}\,K^{-1}}$; $\theta = 0.19\,\mathrm{m^3\,m^{-3}}$; $L = 0.3336 \times 10^6\,\mathrm{J\,kg^{-1}}$; $T_s - T_{fr} = 6\,\mathrm{K}$. No hydrological process is involved in this simulation, which therefore allows the testing of the thermal scheme alone.

Figure 2 displays the progression of the freezing front within the soil as given by the Stefan solution (STEFAN) and by three ORCHIDEE simulations with different configurations: without the freezing scheme and with the default vertical resolution for the thermal module (NOFREEZE; in this case the progression of the 0 °C isotherm is represented); with the freezing scheme and the default vertical resolution for the thermal module (FREEZE, default res.), and with freezing scheme and a refined vertical resolution (FREEZE, improved res.). This resolution was chosen to be the default resolution of the hydrological module (Table 3), and thus only involved the first 2 m of the soil. For those runs the time scale involved did not justify the use of an extended depth for the thermal module.

Both FREEZE simulations obviously improve the modelling of soil thermal dynamics by slowing down the downward progression of the freezing front as compared to NOFREEZE (Fig. 2).

The numerical solutions using the soil freezing scheme show a good agreement with the Stefan solution at the numerical nodes, represented by the dashed lines. However, a net overestimation of the freezing front depth is obvious at depths in-between numerical nodes (step-like features in Fig. 2). It corresponds to a cold bias which increases with depth as the vertical resolution of the model gets coarser. This bias is reduced by the use of a finer resolution (FREEZE, improved res.). The cold bias originates from the linear interpolation of temperatures between the numerical nodes, as illustrated Fig. 3, and can amount up to 25 % of the analytical solution when the default resolution is used. Equivalently, the linear interpolation of a summer temperature

TCD
5, 2197–2252, 2011

profile induces a warm bias and an overestimation of the thawing depth also called active layer. A finer-than-default thermal resolution in the uppermost meters of the soil might therefore improve modelling results for specific applications. However, the use of a coarse resolution does not necessarily affect comparisons with active layer thickness observations as the active layer depth is often diagnosed from a linear interpolation of a measured temperature profile (Brown et al., 2003).

We used the analytical Stefan solution as a benchmark to evaluate the thermal scheme sensitivity to two numerical structural parameters: the vertical discretization and the width of the freezing window ΔT. Romanovsky et al. (1997) underlined the importance but scarcity of such sensitivity analyses for thermal numerical schemes. To fully disentangle spatial from temporal discretization issues, we here consider a fixed time step Δt of 30 min, as it is currently in use for global applications of ORCHIDEE and unlikely to change by a factor more than 2 in near future.

In the absence of issues of numerical stability (see Sect. 1), the model vertical discretization is constrained by the dynamics of the phenomenon it is designed to represent. The real-world phenomenon speed should not exceed the maximum speed of phenomenons representable by the model, i.e. the model speed $v_{\mathrm{mod}} = \frac{\Delta z}{\Delta t}$. Otherwise, part of the observed response will be missed by the model. On the other hand, a model speed much higher than the phenomenon speed will result in a poorly refined representation. In the case of soil freezing we learn from the Stefan analytical solution that the maximum observed speed v_{phen} of the freezing front is reached near the surface during the first time step. With the parameter values in use in this section, $v_{\mathrm{phen}} \sim 4\,\mathrm{cm\,h^{-1}}$ upon a surface forcing of $-6\,^{\circ}\mathrm{C}$. The freezing front progression slows down as deeper soil layers are reached, due to the attenuation of the thermal gradient, so that $v_{\mathrm{phen}} \sim 1\,\mathrm{cm\,h^{-1}}$ at 40 cm below the surface. At the default vertical resolution, $v_{\mathrm{mod}} \sim 8.6\,\mathrm{cm\,h^{-1}}$ just below the surface and $v_{\mathrm{mod}} \sim 40\,\mathrm{cm\,h^{-1}}$ at 40 cm below the surface. The model default time step and vertical resolution are thus adapted to the representation of the dynamics of soil freezing in the first tens of centimeters below the surface; however, the resolution of the process by the model becomes increasingly

TCD
5, 2197–2252, 2011

coarse deeper in the soil. The ideal vertical resolution to capture freezing in the first meter of the soil under a moderate (6 °C) thermal forcing is centimetric.

A second constrain on the spatial discretization arises through the freezing window ΔT: during a time step, a thermal layer crossing the freezing point should not undergo a temperature change $\Delta T_{\mathrm{layer}}$ greater than ΔT during a time step. Otherwise the latent heat energy involved in the phase change would not be accounted for in the model, with consequences for the modelled energy budget and thermal dynamics. Under a given temperature gradient, $\Delta T_{\mathrm{layer}}$ is inversely proportional to the layer heat capacity and thus thickness. Another formulation of the above mentioned constrain is that the finer the spatial discretization, the larger the freezing window should be. Approximating the terms of the Fourier equation, this constrain can be written as:

$$\Delta T_{\mathrm{layer}} < \Delta T$$
$$\frac{K \cdot \nabla T}{C_p \cdot (\Delta z)^2} < \Delta T$$
$$\Delta z > \sqrt{\frac{K \cdot \nabla T}{C_p \cdot \Delta T}} \tag{14}$$

The constrain of Eq. (14) numerically yields $\Delta z > 4$ mm under a temperature forcing of −6 °C and a freezing window of 0.1 °C. However, simulations performed using the default vertical resolution of the model and freezing windows ranging from 2 to 0.1 °C reveal significant errors in the energy budget (Fig. 4). We depict as significant an error in latent heat when it amounts to a quantity of water of the magnitude of the error range in modelled soil water contents, i.e. ∼10 % (Henderson-Sellers, 1996). The freezing window interval can be the source of two types of errors respectively leading to an underestimation (overestimation) of the modelled latent heat: the first one comes from too thin layers undergoing temperature changes of higher magnitude than the freezing window and thus overlooking the phase change. This error is responsible for the latent energy deficit in the uppermost 30 cm of the soil with the $\Delta T = 0.1$ °C freezing window. The second error results from layers whose temperature lies within the freezing window but which undergo a temperature change exceeding the window, thus producing an excess of latent heat in the model. The latent energy overestimation modelled with a $\Delta T = 0.5\,^{\circ}$C freezing window in the uppermost 30 and 60 cm of the soil is an illustration of this second source of error. Both errors can compensate over time, as illustrated by the case $\Delta T = 0.1\,^{\circ}$C: the uppermost thin soil layers overlook the phase change, which leads to a latent heat deficit in the 30 first cm of the soil. The second error dominates then over the deeper, thicker layers and the error in the latent heat budget is almost corrected when the uppermost 60 cm of the soil are considered. Under a given freezing window, excessively thin layers can be subject to both errors with possible compensation over time. This is illustrated by the agreement of the "FREEZE improved res." simulation with the Stefan solution on Fig. 2. Narrow freezing windows and thin layers enhance the freezing-window induced errors; however, the freezing window should be coherent with the physics observed. Based upon these tests, a freezing window of $2\,^{\circ}$C will be used for the rest of this study. A $0.1\,^{\circ}$C-wide freezing window is too small compared to observations (Black and Tice, 1989); a $2\,^{\circ}$C-wide window is all the more realistic as the soil is coarse.

3.2 Test of the freezing scheme against the Mizoguchi experiment

Mizoguchi (1990) performed laboratory experiments of soil freezing designed to monitor the evolution of soil moisture as freezing occurs. Four 20 cm deep soil columns of sand of known properties, with initial uniform water content of 0.33, and in thermal equilibrium at $6.7\,^{\circ}$C, are placed at $t = 0$ under a freezing fluid at $-6\,^{\circ}$C. Only the tops of the columns are sensitive to this boundary condition: the other columns parts are thermally isolated and impermeable. The experiment consists in measuring the soil water distribution after 12, 24 and 48 h of evolution. An unfrozen soil sample serves as a reference.

The Mizoguchi experiments also allow the monitoring of the freezing front progression as it corresponds to the zone the most depleted in water. It hence provides a benchmark for the simulation of temperature and water redistribution as a consequence of freezing, in a simplified context where large-scale effects or precipitation inputs do not add complexity. The Mizoguchi data were exploited by Hansson et al. (2004) for the evaluation of a numerical heat transport and water flow model. The details of the experimental setup and the hydrological parameters values can be found in this publication.

We created an adapted climatologic forcing to test the new soil freezing model against these data. Shortwave radiations were set to zero, incident longwave radiations were chosen as emitted from a blackbody at $-6\,^{\circ}$C. Wind speed was adapted according to the sensible heat flux coefficient transfer mentioned by Hansson et al. (2004). The model was also configured to suit experimental conditions: bottom boundary condition was set to zero drainage; the hydrological soil column was limited to 20 cm; the default hydrological vertical discretization was used; the thermal vertical discretization was refined by a factor two, which prevents from the aforementioned numerical errors while providing a finer resolution over the 20 cm.

Figure 5 compares to the experimental data the modelled freezing front progression and water vertical redistribution resulting from freezing in simulations performed with the new soil freezing scheme using either the linear or thermodynamical parameterization. A control simulation without the freezing scheme was also performed; it lead to a very slight (0.04/20 cm) vertical gradient in water content after 48 h of simulation, as a result of hydro-gravitational equilibrium (not shown).

The modelled and observed progressions of the freezing front (Fig. 5a) agree well with an error less than 6 % at the 3 time-steps where data are available. This confirms the performance of the thermal scheme. We underline that due to parameterization choices, the freezing front progression modelled with the linear and the thermodynamical freezing do not differ (see at the end of this section).

Both the thermodynamical and the linear freezing simulate cryosuction with an amplitude similar to the experimentally observed process (Fig. 5b and c). However, the profiles somehow differ, linear freezing allowing cryosuction to develop deeper within

TCD
5, 2197–2252, 2011

the soil. This can be explained by less drastic a reduction of the liquid water content in the linear freezing when temperature drops below the freezing point (Fig. 1b and c). On the opposite, cryosuction as modelled by the thermodynamical freezing involves greater soil moisture gradients, which results in water movements of stronger magnitude. These simulations alone do not allow to discriminate the performances of one parameterization over the other.

To our knowledge, validations of the soil freezing hydrology of land surface models against cryosuction data are very scarce (e.g. to some extent Koren et al., 1999). The vertical water redistribution resulting from this process impacts the soil thermal properties and thus the frozen soil thermal dynamics, but the parameterization choices we made do not allow to represent this effect, as the soil moisture used by the thermal scheme does not evolve at subfreezing temperature to make energy budget calculations easier. It is also the reason why both soil freezing parameterizations model the same freezing front progression on Fig. 5a. Furthermore, the freezing-induced vertical water redistribution is not expected to have a strong implication after soil thawing: in most regions subject to freezing, saturated conditions are anyway observed and modelled in the uppermost soil in spring as a consequence of snowmelt and/or precipitations infiltration. This may explain the lack of specific validation attempts of land surface hydrological schemes against cryosuction data. Such a validation however appeared to us meaningful to ascertain the model physical realism.

4 Validation against field data at different scales

4.1 Validation at the plot-scale at Valdai

In this section, we use the continuous 18 yr of atmospheric forcing and hydrological data of the Valdai water balance research station (57.6° N, 33.1° E) compiled by Fedorov (1977), Vinnikov et al. (1996) and Schlosser et al. (1997) to evaluate the performances of ORCHIDEE in a region subject to strong seasonal freezing but not underlain

TCD
5, 2197–2252, 2011

by permafrost. These data were extensively used in the PILPS 2d intercomparison project (Schlosser et al., 2000), which provides interesting feedback about biases in the data and other land surface models performances. The long-term hydrological measurements relate to the Usadievskiy experimental catchment, whose 0.36 km^2 areal extent is covered with a grassland meadow. The atmospheric forcing data originate from a grassland plot near the catchment; they were initially sampled at 3-h intervals but we used their 30-min interpolation compiled within the frame of PILPS 2d. The longwave incoming radiations used for our simulation are based on the Idso (1981) algorithm. The observed soil parameters for the catchment are extensively described in Schlosser et al. (1997 and 2000): the ORCHIDEE simulations were performed with a medium soil of rather high hydraulic conductivity (1728 mm d^{-1}) and water holding capacity (401 mm m^{-1}), as prescribed for the PILPS 2d experiment (Schlosser et al., 2000).

Figure 6 compares the mean annual cycles of soil temperature, runoff and soil moisture data over the 18 yr, with ORCHIDEE simulations in three different configurations: without the soil freezing model (NOFREEZE), and with the soil freezing model using the linear parameterization (FREEZE, linear) or the thermodynamical parameterization (FREEZE, thermodynamical). The extended vertical discretization was used for the thermal module.

The new soil freezing model improves the representation of those three variables. The representation of phase change partially corrects the cold bias of ORCHIDEE in winter and totally offsets its warm bias in summer. The choice between a thermodynamical or a linear parameterization of the liquid moisture content does not impact the modeled soil temperature at 20 cm. Each parameterization leads to a slightly different modeled water content for the 20 first cm of the soil; this result means that the soil thermal conductivity and latent energy differences induced are of minor thermal impact. The remaining winter cold bias possibly originates from (i) the underestimation of the snow cover depth in some winters, as assessed from comparisons to in-situ observations (not shown), (ii) a misevaluation of the thermal parameters of the soil, and/or

TCD
5, 2197–2252, 2011

(iii) the use of a constant, uniform and rather high ($0.2\,\mathrm{W\,m^{-1}\,K^{-1}}$) snow conductivity. Summer evaporation (and latent heat exchange over the whole year) is marginally impacted by the introduction of soil freezing; the summer soil cooling modeled in the simulation using the freezing model (FREEZE) originates from a carry-over effect of latent heat consumption during spring thaw in late April. This summer cooling affects the ground below the surface but does not impact the surface temperature itself, which responds to the atmospheric forcing (temperature, radiation).

The timing and amplitude of the runoff spring peak is greatly improved by the soil freezing scheme: the reduced hydraulic conductivity impedes melt water infiltration, and overland flow is generated when the snow melts in April. When the soil freezing module is not used (NOFREEZE), the spring melt water infiltrates into the soil, leading to a soil recharge visible in the 20 first centimeters of the soil (on Fig. 6c). A spring soil recharge of weaker magnitude is recorded in the data, which are averaged from multiple soundings across the catchment (Fig. 6c, DATA). It probably results from macro-scale infiltration pathways still active at subfreezing temperatures and from heterogeneous soil freezing conditions at the scale of the catchment, driven by topography and land cover factors. The soil freezing scheme with linear parameterization is able to reproduce a weak spring soil recharge while the thermodynamical parameterization leads to no recharge at all. In the linear parameterization the reduction of hydraulic conductivity as a function of subfreezing temperature is less drastic and part of the melt water can infiltrate when the temperature is close to the freezing point. The soil recharge modeled by the linear freezing occurs one month later than in data. It corresponds to the timing of the modeled thawing of the soil, which is also delayed when compared to data as reflected by the lag of the modeled spring soil temperature increase Fig. 6a. Considering infiltration, the linear parameterization therefore appears more suited for an integrated description of catchment-scale processes and heterogeneity. Both parameterizations of the freezing capture the autumn runoff peak very well, which occurs as a response of a saturated and/or frozen soil to autumn precipitations.

TCD
5, 2197–2252, 2011

The soil freezing scheme improves the ability of the model to represent the annual amplitude of soil moisture variations. The uppermost soil summer depletion in water is more marked when the soil freezing module is used, because the late thawing of the deeper, quite wet soil layers in June enhances their hydraulic conductivity and thus the drainage towards the deeper soil. When freezing is not accounted for the in-depth soil water profile is closer to hydrodynamic equilibrium and drier at this time of the year, therefore such effects do not occur.

In late autumn (mid-November, December), the magnitude of the observed uppermost soil moisture increase is reproduced when the soil freezing model is used, as a cumulated response to autumn precipitation and first freezing events generating cryosuction. The modeled maximum summer depletion in water occurs in August, one month later than in the observed records. This is correlated to a model bias in evapotranspiration, whose summer maximum displays a one-month lag from the observations (not shown). On average, the soil is wetter than in the observations when the linear parameterization is used, but this is not a meaningful criterion to discriminate the thermodynamical parameterization over the linear one as soil moisture is only modeled in terms of anomaly.

For soil temperature, runoff and soil moisture, the soil freezing module produces an interannual variability of similar amplitude to the data. The modelled winter soil temperature minimums are underestimated due to years where the modelled snow cover is underestimated. The modelled spring runoff minimums are also lower than data minimums due to years when the timing of the runoff spring peak is not captured accurately by the model. The modelled soil moisture variability is greater in spring and autumn than in data: intricated key hydrological processes occur at these times of the year (freezing, thawing, soil subsurface saturation due to precipitation or snow melt), which exhibit a high spatial heterogeneity and are still difficult to capture with a land surface model. Statistics of the modelled and observed interannual variability of soil temperature, moisture and runoff can be found in Table 4. Only the statistics of the thermodynamical parameterization are shown since the linear parameterization leads

Discussion Paper | Discussion Paper | Discussion Paper | Discussion Paper |

TCD

5, 2197–2252, 2011

Multi-scale validation of a new soil freezing scheme

I. Gouttevin et al.

to comparable results. The modelled interannual variability is improved by the use of the soil freezing module in terms of amplitudes and temporal correlation, except for the soil moisture. However, this last parameter exhibits a very low annual interannual variability.

As a conclusion of the Valdai plot-scale model evaluation, the soil freezing scheme noticeably improves the modeled soil thermal and hydrological dynamics at the annual and decadal time-scale; the linear and the thermodynamical parameterizations lead to similar performances, with a slightly better representation of spatially integrated infiltration processes in the linear parameterization.

4.2 Validation across northern Eurasia against soil temperature, active layer and river discharges measurements

We chose to evaluate the new soil freezing model against soil temperature, active layer and river discharges data at the continental scale. Three reasons govern the choice of these variables: (i) they are likely to carry the signature of soil freezing processes; (ii) long-term records exist for them at high latitudes, with an acceptable spatial sampling or spatial representativness (see later in this section); (iii) they are of crucial interest for climate modeling, especially in the prospect of future climate projections. The active layer is the maximal annual thawing depth in permafrost regions. The decomposition of organic matter in high latitude soils majorly occurs within the active layer, which therefore acts as a key control variable of the high northern latitude carbon balance, with implications for future climate projections (Zimov et al., 2006). Frozen soil processes lead to noticeable changes in soil moisture regime (see Sect. 4.1) but in-situ soil moisture observations are very scarce, especially at high northern latitudes, and their spatial representativness is limited (Georgakakos and Baumer, 1996). Conversely, river discharges have been monitored for a long time especially in the former USSR; they provide a spatially integrated information sensitive to the partition between infiltration and runoff at the basin-scale; they constitute a crucial climate variable which models should try to represent accurately, since both the amount and timing of freshwater inflow to the ocean systems are important to ocean circulation salinity and sea ice dynamics (e.g. Peterson et al., 2002).

Our study area is northern Eurasia, ranging from 30° E to 180° E in longitudes, 45° N to 80° N in latitudes. Simulations were performed over this area at a $1^\circ \times 1^\circ$ resolution using the meteorological forcing by Sheffield et al. (2006) for the period 1984–2000, with a 10-yr model spinup forced by the 1983 climatology. The model was run in three different configurations: without the new soil freezing module (NOFREEZE), with the soil freezing module and the linear parameterization (FREEZE, linear) or the thermodynamical parameterization (FREEZE, thermodynamical). The spatialized soil parameters were described in Sect. 1. As the linear and thermodynamical parameterizations did not lead to differences in the modeled thermal regime at the plot-scale (see Sect. 4.1) comparisons related to the thermal regime of the soils were only carried with the thermodynamical parameterization.

4.2.1 Soil temperatures

The comparison of soil temperatures simulated by the model with and without the new soil freezing scheme (Fig. 7) highlights the specific signature of the latent heat effects associated with soil freezing.

The spring cooling due to latent heat consumption as the soil thaws is visible nearly all over Siberia; the soil thawing occurs later (summer) in the areas with the deepest snow cover (North Western Siberia) as the solar radiations first melt the snow. This negative temperature anomaly carries over summer. Its magnitude seems less pronounced over the North Eastern coast of Siberia because "summer" encompasses the month of September where the freezing back of the soil has already occurred in these regions. The soil freezing back is responsible for the autumn warming which first affects the coolest, North-Eastern areas (summer and autumn) and then progresses in the South-Western direction along the thermal gradient (winter). In the coldest, North-Eastern regions the winter soil thermal anomaly inverses due to an opposing mechanism: As ice is thermally more conductivity than water (see Sect. 2), frozen

TCD
5, 2197–2252, 2011

soils are more conductive than unfrozen ones. In regions with shallow snow cover and mean annual ground temperatures well below the freezing point, at the extent of North-Eastern Siberia, the latter effect dominates over the year and leads to a negative annual temperature anomaly upon the introduction of soil freezing. The same phenomenon is observed in regions with very shallow winter snow cover (Gobi desert for instance), where the poor winter thermal insulation helps the cold wave penetrate faster and deeper within the frozen soil. Over regions with milder winter temperatures or thicker snow cover, the warming of winter soil temperature induced by latent heat effects dominates over the year and leads to increased mean annual ground temperatures. Due to the impact of soil freezing on the soil thermal conductivity (and probably also to hydrological feedbacks), soil freezing hence induces an annual thermal effect although the latent heat involved in freezing and thawing balance each other over the year.

In-depth soil temperature is monitored at high northern latitudes as part of the Circumpolar Active Layer Monitoring (CALM, Brown et al., 2003) and the Thermal State of the Permafrost (TSP, IPA-SCIDC, 2010). These datasets respectively include active layer thickness and mean annual ground temperature at different depths. In addition, the Historical Russian Soil Temperature record (HRST, Zhang et al., 2001) provides a historical perspective of the thermal state of the study area.

We compared the soil temperatures simulated by ORCHIDEE with and without freezing to HRST records for the year 1987 at stations spread over our study area (Fig 8), discriminating between the sites where the snow is properly and poorly modeled when compared to observations. The choice of the year 1987 is related to the availability of a global snow depth product (Foster and Davy, 1988) compiled within the ISLSCP Initiative 1 global dataset (Sellers et al., 1996a) for this year.

The new soil freezing scheme degrades the performances of ORCHIDEE in spring and summer, where the spring cooling induced by latent heat consumption increases the model cold bias. This cold bias can be due to the choice of the soil thermal parameters or to the modeled soil moisture content, which affects the soil thermal properties.

However, the new soil freezing scheme helps reducing the model autumn and winter cold bias, especially at the sites where the modeled snow is in relative agreement with observations (agreement within 20 cm, Fig 8). At most other sites, the snow cover is underestimated by the model and the improvement induced by the soil freezing scheme is weaker. At those poorly insulated sites the freezing-induced warming of the soil does not endure over winter as the uppermost soil is strongly influenced by surface temperatures and its thermal conductivity is enhanced. The prominent role of snow in the winter soil thermal regime is confirmed by a forced-snow experiment performed with the soil freezing model at Iakutsk for the year 1987, where the modeled averaged snow depth (10 cm) strongly differs from observations (40 cm). In this experiment we artificially force the model with the observed snow depth and focused on the thermal changes induced (Fig 9): when the observed snow insulates the soil the winter cold bias in modeled soil temperatures is strongly reduced at all depths. The summer cold bias of the “very deep soil” (1 to 3 m) is also reduced, while the shallower soil responds to the surface forcing and does not display a significant bias in both simulations. The poor representation of the Eurasian snow cover could thus be a major cause of the cold bias affecting the modeled soil temperatures. This was already suggested by other modeling groups (Nicolsky et al., 2007; Dankers et al., 2011). The use of a constant and uniform, relatively high thermal conductivity for snow ($0.2\,\mathrm{W\,m^{-1}\,K^{-1}}$) is another possible contributor of this bias: a high thermal snow conductivity may be adapted for a dense tundra snowpack, but the thermal conductivity of taiga snow is known to be far weaker, with typical values of $0.06\,\mathrm{W\,m^{-1}\,K^{-1}}$ (Sturm and Johnsson, 1992). An overestimation of the snow thermal conductivity may explain the degradation of the soil freezing model performances from autumn to winter (Fig. 8).

Finally, recent studies report winter soil temperature increases up to 5 °C upon the introduction of an organic horizon into a land surface model (Rinke et al., 2008; Koven et al., 2009), as this is a dominant feature of the Arctic ecosystems (Beringer et al., 2001). The non representation of this effect in ORCHIDEE may be a supplementary reason for the model winter cold bias.

TCD
5, 2197–2252, 2011

Regarding this analysis, we emphasize that the comparison of model grided outputs to point measurements, as performed here with the HRST network, is of limited relevance due to the extreme spatial variability of soil temperature within a model's grid cell, especially in areas with complex topography (e.g. Leung and Ghan, 1998). As an illustration, the mean annual ground temperature provided for 2008 by the TSP network at 1.5 m at 2 different shallow boreholes distant from ~15 km on the Yamal peninsula differ from 3 K; these two boreholes are located on the same grid cell of the model.

4.2.2 Active layer thickness

Including freezing processes in ORCHIDEE produces an extra-cooling at high northern latitudes, north of 65° N (Fig 7). This decreases the modeled active layer thickness over Eurasia, yielding a better agreement with CALM in-situ observations, especially in Eastern Siberia and over the Yamal peninsula (Fig. 10): the root mean square of the model vs. observation error in the active layer thickness is reduced from 1.9 to 0.5 m. Adding the freezing processes however degrades the results of ORCHIDEE at most Mongolian sites except in the Altaï range. The high spatial variability of the active layer in this region, illustrated by Fig. 10, should be kept in mind when evaluating the model performances; as well as the uncertainties inherent to the comparison of $1^{\circ} \times 1^{\circ}$ model output to point-scale observation reflecting very local climatological and soil conditions. The likely increase in active layer thickness as a response to climate warming at high latitude in the future will enhance soil microbial activity and soil carbone decomposition with impacts on the soil carbon stocks. The modeling of the coupled carbon-climate system at high latitudes is one of the key applications of ORCHIDEE (Koven et al., 2009), which therefore requires realistic simulations of current soil temperatures and active layers.

TCD
5, 2197–2252, 2011

4.2.3 River runoff

Soil freezing exhibits a very specific hydrographical signature in regions at least partially underlain by permafrost: discharges are characterized by very low volumes in winter and a spring peak originating in meltwater which does not infiltrate into weakly permeable, frozen soil. The ability of the new soil freezing module to represent this specific dynamics is evaluated by comparisons between modeled and observed hydrographs at the outflow of the three main Siberian rivers Ob, Ienissei and Lena (Fig. 11). The data originates from the Arctic river discharge database R-ArcticNET (Lammers et al., 2001); comparisons are carried over the 1984–1994 decade, when data is available.

On the three main Siberian basins, the soil freezing processes similarly impact the modeled hydrographs: the reduction of spring water infiltration within the soil leads to a spring peak of runoff concomitant with the timing of snowmelt. The routing of this overland flow towards the mouth of the rivers, performed by the ORCHIDEE routing module, leads to a spring discharge peak whose timing and magnitude are in agreement with the observed discharge peaks at the outflow of the Lena and the Ienissei. On the opposite, meltwater infiltrates within the soil when the physics of soil freezing is not accounted for, and no spring runoff peak is modeled. Drainage occurs at the bottom of the soil, and this subsurface flow sustains the modeled spring discharge peak at the outflow of the rivers. The slower speed of the water flow through subsurface aquifers is responsible for the delay between the spring discharge peaks simulated without and with the soil freezing module, which is also a delay when compared to the observed discharge peaks. We here underline that a spring discharge peak driven by overland flow, as simulated by the soil freezing module, is more reasonable than a drainage-induced spring discharge peak in regions which are partially underlain by permafrost and subject to seasonal freezing. The soil freezing module still does not capture the timing of the spring peak discharge of the Ob river: the vast floodplains of the Ob basin (Ringeval et al., 2010) act as a water reservoir delaying the overland flow

TCD
5, 2197–2252, 2011

in its route towards the outflow of the river. These floodplains are not represented in the soil freezing module and may explain the anticipation of the spring discharge peak modeled at the outflow of the Ob. Other possible causes for this wrong timing might be (i) an anticipated timing of the snowmelt in the Ob basin, which is the most temperate region of the study area; and (ii) the water routing scheme, which was not specifically calibrated for Arctic rivers and does not include ice-jam processes. Those last reasons are however less relevant than the non-representation of floodplains, as only the Ob discharge timing is miscaptured and floodplains are a specific feature of the Ob basin.

The ability of the soil freezing module at capturing the magnitude of the spring discharge peak also varies with the basins and the use of the linear or thermodynamical parameterization. For each river, the linear parameterization leads to a lower spring discharge, because the freezing induced infiltration impedance is less severe in this parameterization and part of the meltwater can infiltrate within the soil and be available for either evapotranspiration or subsurface drainage. For the Ob river, both parameterizations of the soil freezing yield a consequent overestimation of the spring discharge magnitude. This bias is probably partly related to the non-representation of floodplains, which in reality foster large evaporation rates and reduce the amount of the annual water discharge at the mouth of the river. The floodplains water can also infiltrate the soil later in the year and feed some bottom drainage which would maybe maintain a minimum river discharge all year long. This minimum river discharge is clearly underestimated by the soil freezing module with both parameterizations. For the Lena and Ienissei river, the linear parameterization underestimates the magnitude of the spring discharge peak when compared to observations. For the three rivers, the discharge modeled by the linear parameterization also exhibits an unrealistic autumn peak, which originates from bottom drainage at the time of the year where the summer heat wave reaches the bottom of the soil column (2 m) and partly melts the water there, locally increasing the hydraulic conductivity of the soil. This feature is less visible for the Lena basin which is overall colder than the Ienissei and Ob regions so that soil bottom melting does not occur in autumn; it is also less pronounced with the thermodynamical

TCD
5, 2197–2252, 2011

parameterization for all three basins, because warming closer to the freezing point is required to melt part of the water in this formulation.

The inability of the soil freezing model at capturing the minimum winter discharges highlights one of its possible weaknesses. When the soil freezing module is used, autumn rain or melt water hardly infiltrates into the already partially frozen soil, and overland flow is produced. In reality, the soil temperatures and thus frozen or unfrozen states exhibits a high spatial variability at the model grid-cell scale (e.g. Leung and Ghan, 1998), and at this scale, part of the water can infiltrate, though with reduced efficiency (e.g. Cherkauer and Lettenmeier, 2003; Niu and Yang, 2006). Taking this subgrid variability into account is likely to sustain a winter, drainage-induced discharge, as simulated when the soil freezing module is not used. The Lena river discharge modeled by the soil freezing module is less affected by this bias: more than 78 % of the Lena basin is underlain by permafrost (Serreze et al., 2002), compared to respectively 36 % and 4 % for the Ienissei and the Ob basins. Accounting for a subgrid variability in the frozen status of the soil is less crucial in the Lena basin since the soil is homogeneously frozen most of the year.

Overall the new soil freezing module better represents the processes governing the Siberian rivers annual dynamics. It yields a good agreement between modeled discharges and in-situ data. The thermodynamical parameterization appears more suited for large scale applications. A subgrid variability approach and the representation of wetlands are diagnosed as necessary to capture the annual cycle of the Arctic river discharges with more accuracy.

5 Conclusion and outlook

A new soil freezing scheme including a multi-layer hydrology was implemented into the land-surface scheme ORCHIDEE, designed to run within the global climate model IPSL CM4. Combining frozen soil processes with a vertically detailed hydrology is crucial for the modeling of the carbon-cycle in the Arctic and future climate projections.

The thermal and hydrological behaviors of the new soil freezing scheme are validated at different scales. This scheme thoroughly improves the modeling of the soil temperature and hydrology at the small and intermediate scales in regions subject to freezing. At the continental scale, it only partially corrects a winter cold bias in soil temperatures, which is partly imputed to the inaccuracy of snow modeling and the non-representation of organic matter. These points are therefore the focus of current developing work. The soil freezing processes also yield a more reasonable representation of the active layer, which governs most of the carbon decomposition processes and is therefore a key variable of the carbon-cycle at high latitudes. The freezing scheme catches with an increased accuracy the specific features of the hydrological regime of Siberian rivers in regions underlain by permafrost. However, the representation of wetlands and the use of a subgrid variability approach appear necessary, especially in regions undergoing seasonal freezing. It will constitute the focus of further developments.

Acknowledgements. This research was supported by the European FP7 project COMBINE and by the project CLASSIC, funded by the Agence Nationale pour la Recherche (ANR).

INSU
Institut national des **sciences** de **l'Univers**

The publication of this article is financed by CNRS-INSU.

References

Abu-Hamdeh, N. and Reeder, R.: Soil thermal conductivity : Effects of density, moisture, salt concentration, and organic matter, Soil Sci. Soc. Am. J., 64, 1285–1290, 2000.

Adam, J. and Lettenmaier, D.: Adjustment of global gridded precipitation for systematic bias, J. Geophys. Res., 108, 4257, doi:10.1029/2002JD002499, 2003.

Alexeev, V., Nicolsky, D., Romanovsky, V., and Lawrence, D.: An evaluation of deep soil configurations in the CLM3 for improved representation of permafrost, Geophys. Res. Lett., 34, L09502, doi:10.1029/2007GL029536, 2007.

Anisimov, O. and Nelson, F.: Permafrost zonation and climate change in the northern hemisphere: results from transient general circulation models, Climatic Change, 35, 241–258, doi:10.1023/A:1005315409698, 1997.

Arnell, N.: Implications of climate change for freshwater inflows to the Arctic Ocean, J. Geophys. Res., 110, D07105, doi:10.1029/2004JD005348, 2005.

Barry, R. and Serreze, M. : Atmospheric components of the Arctic Ocean freshwater balance and their interannual variability, The Freshw. Budg. Arct. Ocean., 45–56, 2000.

Beringer, J., Lynch, A., Chapin III, F., Mack, M., and Bonan, G. : The representation of Arctic Soils in the Land Surface Model: The Importance of Mosses, J. Climate., 14, 3324–3335, doi:10.1175/1520-0442(2001)014<3324:TROASI>2.0.CO;2, 2001.

Black, P. and Tice, A.: Comparison of soil freezing curve and soil water curve data for Windsor sandy loam, Water Resour. Res., 25, 2205–2210, doi:10.1029/WR025i010p02205, 1989.

Boike, J., Roth, K., and Overduin, P.: Thermal and hydrologic dynamics of the active layer at a continuous permafrost site (Taymyr Peninsula, Siberia), Water Resour. Res., 34, 355–363, doi:10.1029/97WR03498, 1998.

Bonan, G., Oleson, K., Vertenstein, M., Levis, S., Zeng, X., Dai, Y., Dickinson, R., and Yang, Z.: The Land Surface Climatology of the Community Land Model Coupled to the NCAR Community Climate Model, J. Climate., 15, 3123–3149, doi:10.1175/1520-0442(2002)015<3123:TLSCOT>2.0.CO;2, 2002.

Brown, J., Hinkel, K., and Nelson, F. (compilers): Circumpolar Active Layer Monitoring (CALM) program network: description and data, International Permafrost Association Standing Committee on Data Information and Communication, 2003.

Burt, T. and Williams, P.: Hydraulic conductivity in frozen soils, Earth Surf. Processes, 1, 349–360, 1976.

Carsel, R. and Parrish, R.: Developing joint probability distributions of soil water retention characteristics, Water Resour. Res., 24, 755–769, doi:10.1029/WR024i005p00755, 1988.
Cherkauer, K. and Lettenmaier, D.: Hydrologic effects of frozen soils in the upper Mississippi River basin, J. Geophys. Res., 104, 19599, doi:10.1029/1999JD900337, 1999.
Cherkauer, K. and Lettenmaier, D.: Simulation of spatial variability in snow and frozen soil, J. Geophys. Res., 108, 10–1029, doi:10.1029/2003JD003575, 2003.
Choisnel, E.: Le bilan d'énergie et le bilan hydrique du sol, La Météorologie, 6, 103–133, 1977.
Cox, P., Betts, R., Bunton, C., Essery, R., Rowntree, P., and Smith, J.: The impact of new land surface physics on the GCM simulation of climate and climate sensitivity, Clim. Dynam., 15, 183–203, doi:10.1007/s003820050276, 1999.
Dall'Amico, M.: Coupled Water and Heat Transfer in Permafrost Modeling, Ph.D. thesis, University of Trento, 2010.
Dankers, R., Burke, E. J., and Price, J.: Simulation of permafrost and seasonal thaw depth in the JULES land surface scheme, The Cryosphere Discuss., 5, 1263–1309, doi:10.5194/tcd-5-1263-2011, 2011.
De Rosnay, P. and Laval, K. : Representation of soil-vegetation-atmosphere interaction in the general circulation model of the Laboratoire de Météorologie Dynamique, Ph.D. thesis, Université de Paris VI, 1999.
De Vries, D. A.: Thermal properties of soils, in: Physics of Plant Environment, edited by: van Wijk, W. R., North Holland, Amsterdam, 1963.
Dominé, F., Taillandier, A., Houdier, S., Parrenin, F., Simpson, W., and Douglas, T.: Interactions between snow metamorphism and climate: Physical and chemical aspects, Physics and Chemistry of Ice, edited by: Kuhs, W. F., Royal Society of Chemistry, UK, Cambridge, 27–46, 2007.
Dooge, J. and Bruen, M.: Scaling effects on moisture fluxes at unvegetated land surfaces, Water Resour. Res., 33, 2923–2927, doi:10.1029/97WR01709, 1997.
d'Orgeval, T., Polcher, J., and de Rosnay, P.: Sensitivity of the West African hydrological cycle in ORCHIDEE to infiltration processes, Hydrol. Earth Syst. Sci., 12, 1387–1401, doi:10.5194/hess-12-1387-2008, 2008.
Essery, R., Best, M., and Cox, P.: MOSES 2.2 technical documentation, Hadley Centre technical note, 30, 1–31, 2001.
Farouki, O.: The thermal properties of soils in cold regions, Cold Reg. Sci. Technol., 5, 67–75, doi:10.1016/0165-232X(81)90041-0, 1981.

TCD
5, 2197–2252, 2011

Multi-scale validation of a new soil freezing scheme

I. Gouttevin et al.

Fedorov, S.: A Study of the Components of the Water Balance in Forest Zone of European Part of the USSR, Gidrometeoizdat, St Petersbourg, 264 pp., 1977.
Foster, D. and Davy, R.: Global snow depth climatology., Tech. rep., USAFETAC/TN-88/006, Scott Air Force Base, Illinois, 1988.
Fuchs, M., Campbell, J., and Papendick, R.: An Analysis of Sensible and Latent Heat Flow in a Partially Frozen Unsaturated Soil1, Soil Sci. Soc. Am. J., 42, 379–385, 1978.
Georgakakos, K. and Baumer, O.: Measurement and utilization of on-site soil moisture data, J. Hydrol., 184, 131–152, doi:10.1016/0022-1694(95)02971-0, 1996.
Hansson, K., Simunek, J., Mizoguchi, M., Lundin, L., and Van Genuchten, M.: Water flow and heat transport in frozen soil: Numerical solution and freeze-thaw applications, Vadose Zone J., 3, 693–704, 2004.
Henderson-Sellers, A.: Soil moisture simulation: Achievements of the RICE and PILPS intercomparison workshop and future directions, Global Planet. Chang., 13, 99–115, doi:10.1016/0921-8181(95)00035-6, 1996.
Hourdin, F.: Study and numerical simulation of the general circulation of planetary atmospheres, Ph.D. thesis, Université de Paris VII, 1992.
Idso, S. B.: A set of equations for full spectrum and 8–14 µm and 10.5–12.5 µm thermal radiation from cloudless skies, Water Resour. Res., 17, 295–304, doi:10.1029/WR017i002p00295, 1981.
IPA SCDIC (International Permafrost Association Standing Committee for Data, Information and Communication): The IPY Thermal State of Permafrost (TSP) Snapshot Borehole Inventory, available at: http://nsidc.org/, 2010.
Johansen, O.: Thermal conductivity of soils, Ph.D. thesis, Trondheim, Norway, 1975.
Kane, D.: The Impact of Hydrologic Perturbation on Arctic Ecosystems Induced by Climate Change, Global Change and Arctic Terrestrial Ecosystems, Ecological Studies, 124, 63–81, 1997.
Khvorostyanov, D., Ciais, P., Krinner, G., Zimov, S., Corradi, C., and Guggenberger, G.: Vulnerability of permafrost carbon to global warming. Part II : sensitivity of permafrost carbon stock to global warming, Tellus B, 60, 265–275, doi:10.1111/j.1600-0889.2007.00336.x, 2008.
Koopmans, R. and Miller, R.: Soil freezing and soil water characteristic curves, Soil Sci. Soc. Am. Pro., 30, 680–685, 1966.
Koren, V., Schaake, J., Mitchell, K., Duan, Q., Chen, F., and Baker, J.: A parameterization of snowpack and frozen ground intended for NCEP weather and climate models, J. Geophys.

Res., 104, 19569, doi:10.1029/1999JD900232, 1999.

Koven, C., Friedlingstein, P., Ciais, P., Khvorostyanov, D., Krinner, G., and Tarnocai, C.: On the formation of high-latitude soil carbon stocks : Effects of cryoturbation and insulation by organic matter in a land surface model, Geophys. Res. Lett., 36, L21501, doi:10.1029/2009GL040150, 2009.

Kowalczyk, E., Wang, Y., Law, R., Davies, H., McGregor, J., and Abramowitz, G.: The CSIRO Atmosphere Biosphere Land Exchange (CABLE) model for use in climate models and as an offline model, CSIRO Marine and Atmospheric Research Paper 013, 42 pp., Aspendale, Australia, 2006.

Krinner, G., Viovy, N., de Noblet-Ducoudré, N., Ogée, J., Polcher, J., Friedlingstein, P., Ciais, P., Sitch, S., and Prentice, I.: A dynamic global vegetation model for studies of the coupled atmosphere-biosphere system, Global Biogeochem. Cy., 19, GB1015, doi:10.1029/2003GB002199, 2005.

Lammers, R., Shiklomanov, A., Vörösmarty, C., Fekete, B., and Peterson, B.: Assessment of contemporary Arctic river runoff based on observational discharge records, J. Geophys. Res., 106, 3321–3334, doi:10.1029/2000JD900444, 2001.

Lawrence, D. and Slater, A.: A projection of severe near-surface permafrost degradation during the 21st century, Geophys. Res. Lett., 32, L24401, doi:10.1029/2005GL025080, 2005.

Leung, L. and Ghan, S.: Parameterizing subgrid orographic precipitation and surface cover in climate models, Mon. Weather Rev., 126, 3271–3291, 1998.

Li, X. and Koike, T.: Frozen soil parameterization in SiB2 and its validation with GAME-Tibet observations, Cold Reg. Sci. Technol., 36, 165–182, doi:10.1016/S0165-232X(03)00009-0, 2003.

Lundin, L.: Hydraulic properties in an operational model of frozen soil, J. Hydrol., 118, 289–310, doi:10.1016/0022-1694(90)90264-X, 1990.

Luo, L., Robock, A., Vinnikov, K., Schlosser, C., Slater, A., Boone, A., Etchevers, P., Habets, F., Noilhan, J., Braden, H., Cox, P., De Rosnay, P., Dickinson, R., Dai, Y., Duan, Q., Etchevers, P., Henderson-Sellers, A., Gedney, N., Gusev, Y., Habets, F., Kim, J., Kowalczyk, E., Mitchell, K., Nasonova, O., Noilhan, J., Pitman, A., Schaake, J., Shmakin, A., Smirnova, T., Wetzel, P., Xue, Y., Yang, Z., and Zeng, Q: Effects of frozen soil on soil temperature, spring infiltration, and runoff: Results from the PILPS 2 (d) experiment at Valdai, Russia, J. Hydrometeorol., 4, 334–351, doi:10.1175/1525-7541(2003)4<334:EOFSOS>2.0.CO;2, 2003.

Macdonald, R., Carmack, E., McLaughlin, F., Falkner, K., and Swift, J.: Connections among ice, runoff and atmospheric forcing in the Beaufort Gyre, Geophys. Res. Lett., 26, 2223–2226, doi:10.1029/1999GL900508, 1999.

Mackay, J.: The world of underground ice, Annals Assoc. Am. Geogr., 62, 1–22, 1972.

Mizoguchi, M.: Water, heat and salt transport in freezing soil, Ph.D. thesis (in Japanese), University of Tokyo, 1990.

Mualem, Y.: A new model for predicting the hydraulic conductivity of unsaturated porous media, Water Resour. Res., 12, 513–522, 1976.

Ngo-Duc, T., Laval, K., Ramillien, G., Polcher, J., and Cazenave, A.: Validation of the land water storage simulated by Organising Carbon and Hydrology in Dynamic Ecosystems (ORCHIDEE) with Gravity Recovery and Climate Experiment (GRACE) data, Water Resour. Res., 43, W04427, doi:10.1029/2006WR004941, 2007.

Nicolsky, D., Romanovsky, V., Alexeev, V., and Lawrence, D.: Improved modelling of permafrost dynamics in a GCM land-surface scheme, Geophys. Res. Lett., 34, L08501, doi:10.1029/2007GL029525, 2007.

Niu, G. and Yang, Z.: Effects of frozen soil on snowmelt runoff and soil water storage at a continental scale, J. Hydrometeorol., 7, 937–952, 2006.

Nobrega, S. and Grogan, P.: Deeper snow enhances winter respiration from both plant-associated and bulk soil carbon pools in birch hummock tundra, Ecosystems, 10, 419–431, 2007.

Osterkamp, T. and Romanovsky, V.: Freezing of the active layer on the coastal plain of the Alaskan Arctic, Permafrost Periglac., 8, 23–44, 1997.

Peterson, B., Holmes, R., McClelland, J., Vörösmarty, C., Lammers, R., Shiklomanov, A., Shiklomanov, I., and Rahmstorf, S.: Increasing river discharge to the Arctic Ocean, Science, 298, 2171–2173, doi:10.1126/science.1077445, 2002.

Pielke, R.: Mesoscale meteorological modeling, Academic Press, Elsevier, San Diego (CA), 2001.

Pitman, A., Slater, A., Desborough, C., and Zhao, M.: Uncertainty in the simulation of runoff due to the parameterization of frozen soil moisture using the Global Soil Wetness Project methodology, J. Geophys. Res., 104, 16, 16879–16888, 1999.

Quinton, W., Shirazi, T., Carey, S., and Pomeroy, J.: Soil water storage and active-layer development in a sub-alpine tundra hillslope, southern Yukon Territory, Canada, Permafrost Periglac., 16, 369–382, 2005.

Ringeval, B., de Noblet-Ducoudré, N., Ciais, P., Bousquet, P., Prigent, C., Papa, F., and Rossow,

W. B.: An attempt to quantify the impact of changes in wetland extent on methane emissions on the seasonal and interannual time scales, Global Biogeochem. Cy., 24, GB2003, doi:10.1029/2008GB003354, 2010.
Ringeval, B., Decharme, B., Piao, S., Ciais, P., Papa, F., de Noblet-Ducoudré, N., Prigent, C., Friedlingstein, P., Gouttevin, I., and Koven, C.: Modelling sub-grid soil moisture saturation in the ORCHIDEE global land surface model: Evaluation against river discharges and remotely sensed data, submitted, 2011.
Rinke, A., Kuhry, P., and Dethloff, K.: Importance of a soil organic layer for Arctic climate: A sensitivity study with an Arctic RCM, Geophys. Res. Lett., 35, L13709, doi:10.1029/2008GL034052, 2008.
Romanovsky, V. and Osterkamp, T.: Effects of unfrozen water on heat and mass transport processes in the active layer and permafrost, Permafrost Periglac., 11, 219–239, 2000.
Romanovsky, V., Osterkamp, T., and Duxbury, N.: An evaluation of three numerical models used in simulations of the active layer and permafrost temperature regimes, Cold Reg. Sci. Technol., 26, 195–203, 1997.
Schlosser, C., Robock, A., Vinnikov, K., Speranskaya, N., and Xue, Y.: 18-year landsurface hydrology model simulations for a midlatitude grassland catchment in Valdai, Russia, Mon. Weather. Rev., 125, 3279–3296, 1997.
Schlosser, C., Slater, A., Pitman, A., Robock, A., Vinnikov, K., Henderson-Sellers, A., Speranskaya, N., and Mitchell, K. : Simulations of a boreal grassland hydrology at Valdai, Russia: PILPS Phase 2 (d), Mon. Weather. Rev., 128, 301–321, 2000.
Sellers, P., Meeson, B., Closs, J., Collatz, J., Corprew, F., Dazlich, D., Hall, F., Kerr, Y., Koster, R., Los, S., Mitchell, K., McManus, J., Myer, D., Sun, K., and Try, P: The ISLSCP Initiative I global datasets : Surface boundary conditions and atmospheric forcings for land-atmosphere studies, B. Am. Meteorol. Soc., 77, 1987–2005, 1996a.
Sellers, P., Randall, D., Collatz, G., Berry, J., Field, C., Dazlich, D., Zhang, C., Collelo, G., and Bounoua, L.: A revised land surface parameterization (SiB2) for atmospheric GCMs. Part I: Model formulation, J. Climate, 9, 676–705, 1996b.
Serreze, M., Walsh, J., Chapin, F., Osterkamp, T., Dyurgerov, M., Romanovsky, V., Oechel, W., Morison, J., Zhang, T., and Barry, R. : Observational evidence of recent change in the northern high-latitude environment, Climatic Change, 46, 159–207, 2000.
Serreze, M., Bromwich, D., Clark, M., Etringer, A., Zhang, T., and Lammers, R.: Large-scale hydro-climatology of the terrestrial Arctic drainage system, J. Geophys. Res., 108, 8160,

doi:10.1029/2001JD000919, 2003.
Sheffield, J., Goteti, G., and Wood, E.: Development of a 50-year high-resolution global dataset of meteorological forcings for land surface modeling, J. Climate, 19, 3088–3111, 2006.
Slater, A., Pitman, A., and Desborough, C.: Simulation of freeze-thaw cycles in a general circulation model land surface scheme, J. Geophys. Res., 103, 11303–11312, 1998.
Smirnova, T., Brown, J., Benjamin, S., and Kim, D.: Parameterization of cold-season processes in the MAPS land-surface scheme, J. Geophys. Res., 105, 4077–4086, 2000.
Solomon, S., Qin, D., Manning, M., Chen, Z., Marquis, M., Averyt, K., Tignor, M., and Miller, H.: IPCC, 2007: Climate change 2007: The physical science basis. Contribution of Working Group I to the fourth assessment report of the Intergovernmental Panel on Climate Change, 2007.
Stefan, J.: Über die Theorie der Eisbildung, Monatsh. Math., 1, 1–6, 1890.
Stendel, M. and Christensen, J.: Impact of global warming on permafrost conditions in a coupled GCM, Geophys. Res. Lett., 29, 1632, doi:10.1029/2001GL014345, 2002.
Sturm, M. and Johnson, J.: Thermal conductivity measurements of depth hoar, J. Geophys. Res., 97, 2129–2139, doi:10.1029/91JB02685, 1992.
Takata, K. and Kimoto, M.: A numerical study on the impact of soil freezing on the continental-scale seasonal cycle, J. Meteorol. Soc. Jpn., 78, 199–221, 2000.
Tarnocai, C., Canadell, J., Schuur, E., Kuhry, P., Mazhitova, G., and Zimov, S.: Soil organic carbon pools in the northern circumpolar permafrost region, Global Biogeochem. Cycles., 23, GB2023, doi:10.1029/2008GB003327, 2009.
Van Genuchten, M.: A closed-form equation for predicting the hydraulic conductivity of unsaturated soils, Soil Sci. Soc. Am. J., 44, 892–898, 1980.
Verseghy, D. L.: CLASS – A Canadian land surface scheme for GCMs. I. Soil model, Int. J. Climatol., 11, 111–133, 1991.
Vinnikov, K. Y., Yeserkepova, I. B., Robock, A., Speranskaya, N. A., and Schlosser, C. A.: Scales of temporal and spatial variability of midlatitude soil moisture, J. Geophys. Res., 101, 7–174, 1996.
Williams, P. and Smith, M.: The frozen Earth: fundamentals of geocryology, Cambridge University Press Cambridge, 1989.
Woo, M., Marsh, P., and Pomeroy, J.: Snow, frozen soils and permafrost hydrology in Canada, 1995–1998, Hydrol. Process., 14, 1591–1611, 2000.
Xue, Y., Zeng, F., and Adam Schlosser, C.: SSiB and its sensitivity to soil properties – a case

study using HAPEX-Mobilhy data, Global Planet. Change, 13, 183–194, 1996.
Yang, D., Kane, D., Hinzman, L., Zhang, X., Zhang, T., and Ye, H.: Siberian Lena River hydrologic regime and recent change, J. Geophys. Res., 107(4), 4694, doi:10.1029/2002JD002542, 2002.
Yi, S., Arain, M., and Woo, M.: Modifications of a land surface scheme for improved simulation of ground freeze-thaw in northern environments, Geophys. Res. Lett., 33, L13501, doi:10.1029/2006GL026340, 2006.
Zhang, T., Barry, R., and Gilichinsky, D. (compilers): Russian historical soil temperature data, 2001, updated 2006. Boulder, Colorado USA: National Snow and Ice Data Center. Digital media, 2001.
Zhang, T., Barry, R., Knowles, K., Ling, F., and Armstrong, R.: Distribution of seasonally and perennially frozen ground in the Northern Hemisphere, in: Proceedings of the 8th International Conference on Permafrost, 21–25 July 2003, Zurich, Switzerland, 1289–1294, 2003.
Zobler, L.: A world soil file for global climate modeling, NASA technical memorandum, 87802, 1986.

Table 1. Soil types and their hydraulic characteristics in ORCHIDEE.

Soil type	USDA name	K_s (mm d^{-1})	α (m^{-1})	θ_s	θ_r	n
coarse	Sandy loam	1060.8	1.89	0.41	0.065	7.5
medium	Medium loam	249.6	1.56	0.43	0.078	3.6
fine	Clay loam	62.4	1.31	0.41	0.095	1.9

TCD
5, 2197–2252, 2011

TCD
5, 2197–2252, 2011

Multi-scale validation of a new soil freezing scheme

I. Gouttevin et al.

Table 2. Values of the thermal parameters used in ORCHIDEE.

Thermal conductivities ($W\,m^{-1}\,K^{-1}$)		Heat capacities ($\times 10^6\,J\,m^{-3}\,K^{-1}$)	
k_s	2.32		
k_i	2.2	C_{icy}	2.3
k_w	0.6	C_{wet}	3.03
k_{dry}	0.4	C_{dry}	1.8

Table 3. Numerical nodes of the thermal and hydrological modules in the default configuration, and in the extended-depth configuration for the thermal module of the new soil freezing scheme.

Layer no.	Depth of the numerical nodes (cm)		
	Thermal module		Hydrological module
	Default resolution	Extended depth	
1	1.8	1.8	0.05
2	7.9	7.9	0.19
3	20	20	0.4
4	44	44	0.9
5	93	93	2
6	1.91	1.91	4.2
7	3.86	3.86	8.7
8		7.76	17.5
9		15.6	35
10		31.2	70
11		62.4	141

TCD
5, 2197–2252, 2011

Table 4. Standard deviation σ and correlation coefficient r between model (FREEZE, thermodynamical) and data for the 20 cm soil temperature, runoff and 20 cm soil moisture over the 18 yr of simulations and data available at Valdai. For each time period the statistics are computed using the modeled or observed value averaged over the time period. The statistics improved by the use of the soil freezing module are highlighted.

	20 cm soil temperature (°C)						Runoff (mm/period)						20 cm soil moisture (–)					
	annual		winter		summer		annual		spring		autumn		annual		winter		summer	
	σ	r	σ	r	σ	r	σ	r	σ	r	σ	r	σ	r	σ	r	σ	r
data	1.18		1.0		0.9		91		60		49		0.05		0.08		0.1	
nofreeze	1.5	0.44	1.9	0.7	1	0.9	64	0.57	34	0.25	15	0.59	0.01	0.57	0.01	0.5	0.03	0.85
freeze	**1.45**	**0.44**	**0.9**	0.68	**0.9**	**0.9**	**78**	**0.70**	**74**	**0.69**	**37**	**0.78**	**0.02**	0.30	**0.03**	0.25	**0.03**	0.7

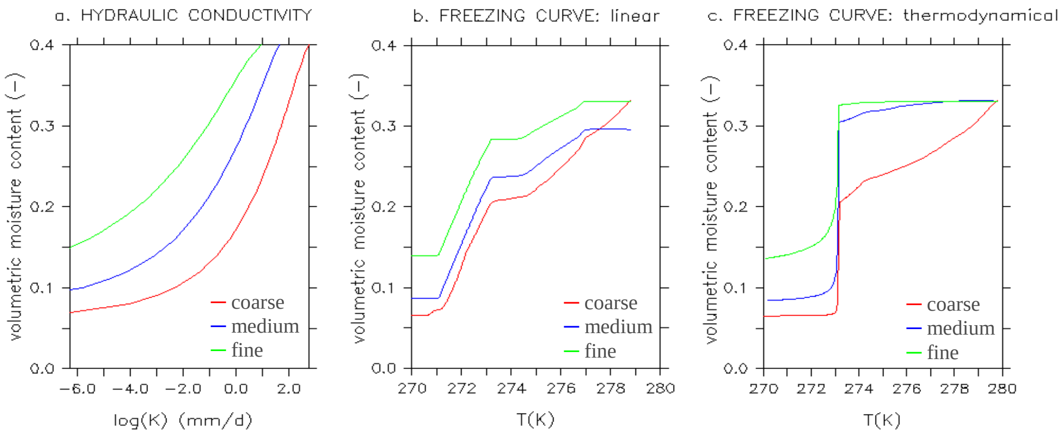

Fig. 1. **(a)** Hydraulic conductivities of the three soil types (fine, medium, coarse) represented in ORCHIDEE. **(b)** Liquid water content as a function of temperature as simulated with the LINEAR freezing for those three soil types. Initial soil volumetric moisture content and temperature were 0.33 and 280 K. **(c)** Same as **(b)** but for THERMODYNAMICAL freezing.

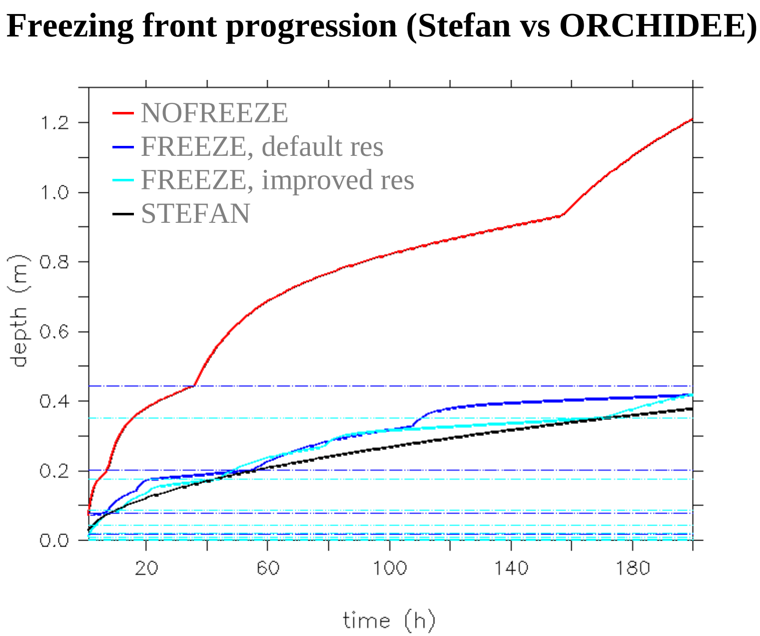

Fig. 2. Freezing front progression as calculated by the Stefan solution (STEFAN) and simulated by three ORCHIDEE simulations: without soil-freezing (NOFREEZE); with the soil-freezing thermal algorithm at the default resolution (FREEZE, default res.), and with the soil-freezing thermal algorithm at an improved resolution (FREEZE, improved res.). The horizontal dashed lines mark the positions of the vertical nodes in the different resolutions.

TCD
5, 2197–2252, 2011

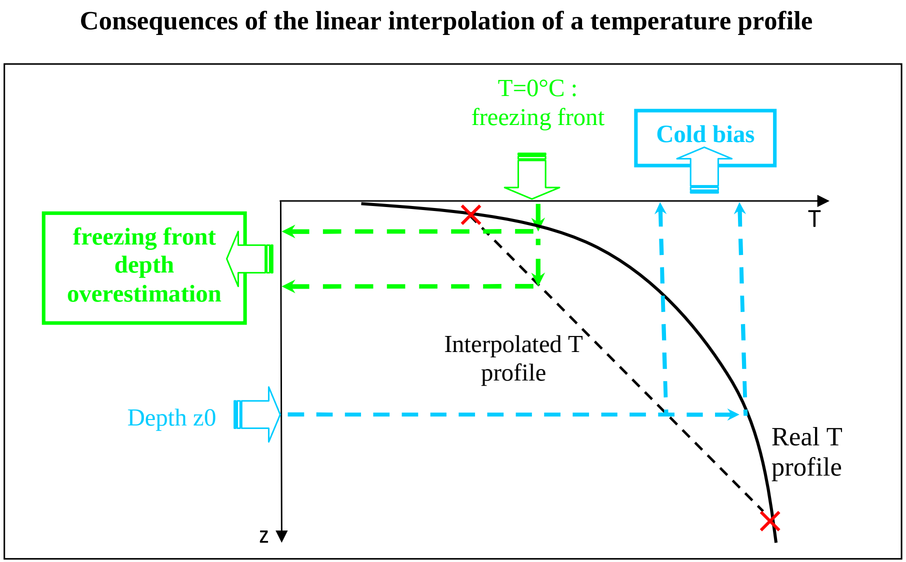

Fig. 3. Consequences of the linear interpolation (black, dash) of a temperature profile (black) in-between vertical nodes. The linear interpolation of a winter profile leads to a systematic overestimation of the freezing front depth, or equivalently, a cold bias between thermal nodes.

TCD
5, 2197–2252, 2011

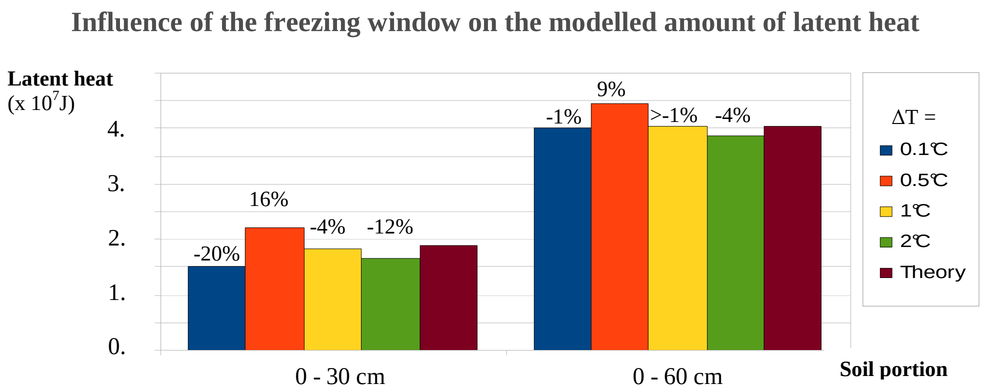

Fig. 4. Latent heat energy involved in the phase change upon the freezing of the first 30 (left) and 60 (right) cm of the soil for different ORCHIDEE simulations referenced by the width of their freezing window (0.1 to 2 °C) and theoretically calculated for the corresponding water amount (Theory). The relative error to Theory is mentioned at the top of each simulation column.

TCD
5, 2197–2252, 2011

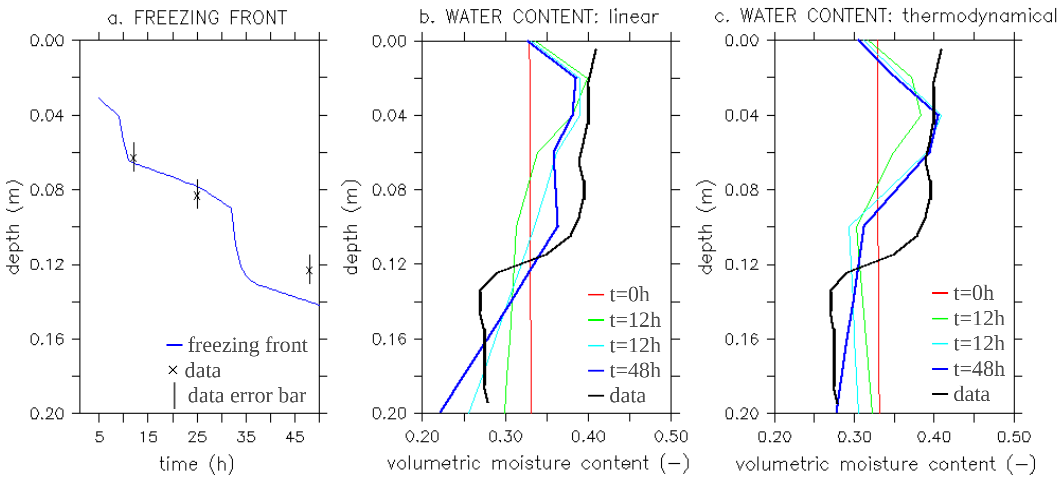

Fig. 5. Comparison of observed and modelled freezing front progression and cryosuction. **(a)** Modelled freezing front progression (blue) and experimental data (points) with afferent error bars. The freezing front progression modelled with the linear and the thermodynamical freezing do not differ. **(b)**, **(c)** Total (frozen + unfrozen) water content evolution within the soil column at different time steps, for the linear **(b)** and thermodynamical **(c)** parameterizations of the freezing. The modelled water content at 48 h (blue, thick) is to compare to the data at the same time step (black, thick).

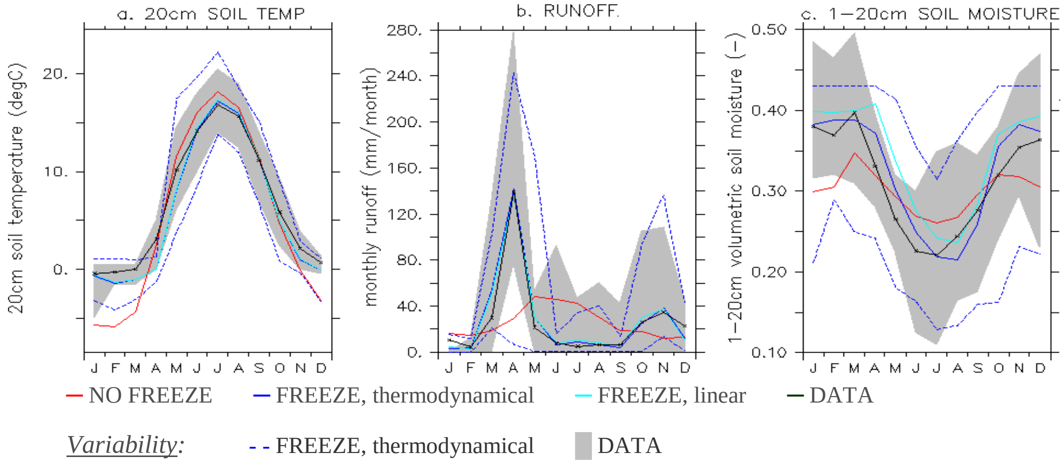

Fig. 6. Annual cycles of monthly mean 20 cm soil temperature **(a)**, monthly mean runoff **(b)** and monthly mean 1–20 cm soil moisture **(c)** simulated by ORCHIDEE with (FREEZE) and without (NOFREEZE) the freezing scheme, and compared with available data (DATA) over 1966–1983. The grey and the dashed blue envelopes respectively represent the annual variability in data and in the FREEZE, thermodynamical simulation.

TCD

5, 2197–2252, 2011

Multi-scale validation of a new soil freezing scheme

I. Gouttevin et al.

Title Page
Abstract | Introduction
Conclusions | References
Tables | Figures
◀| |▶
◀ ▶
Back | Close
Full Screen / Esc
Printer-friendly Version
Interactive Discussion

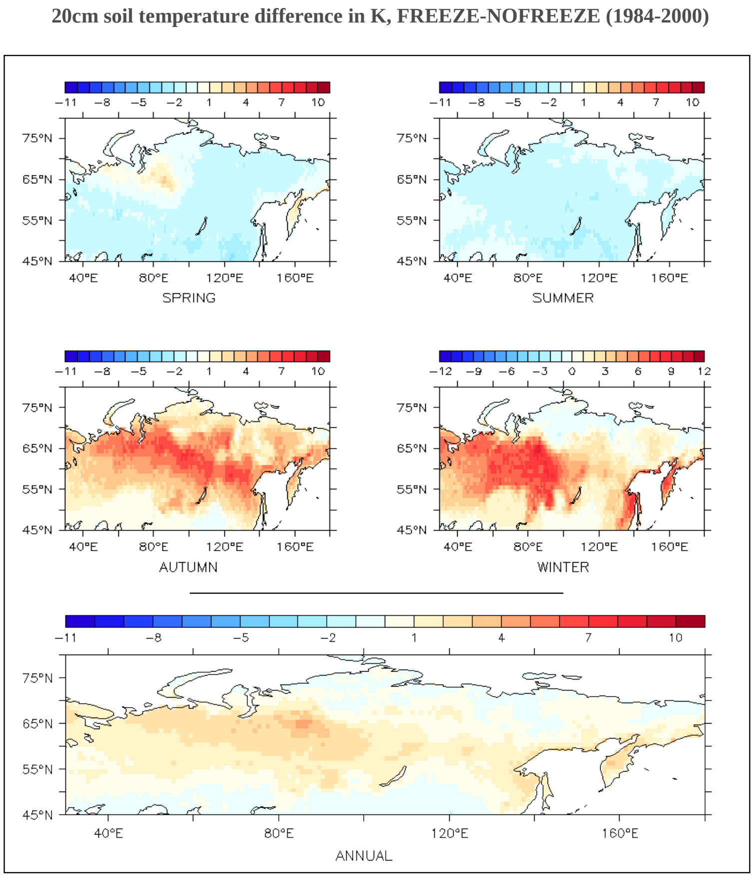

Fig. 7. 20 cm soil temperature difference between the model with and without the new soil freezing scheme. Top: seasonal averages over the (1984–2000) period. Bottom: annual average over the (1984–2000) period.

TCD
5, 2197–2252, 2011
Multi-scale validation of a new soil freezing scheme
I. Gouttevin et al.

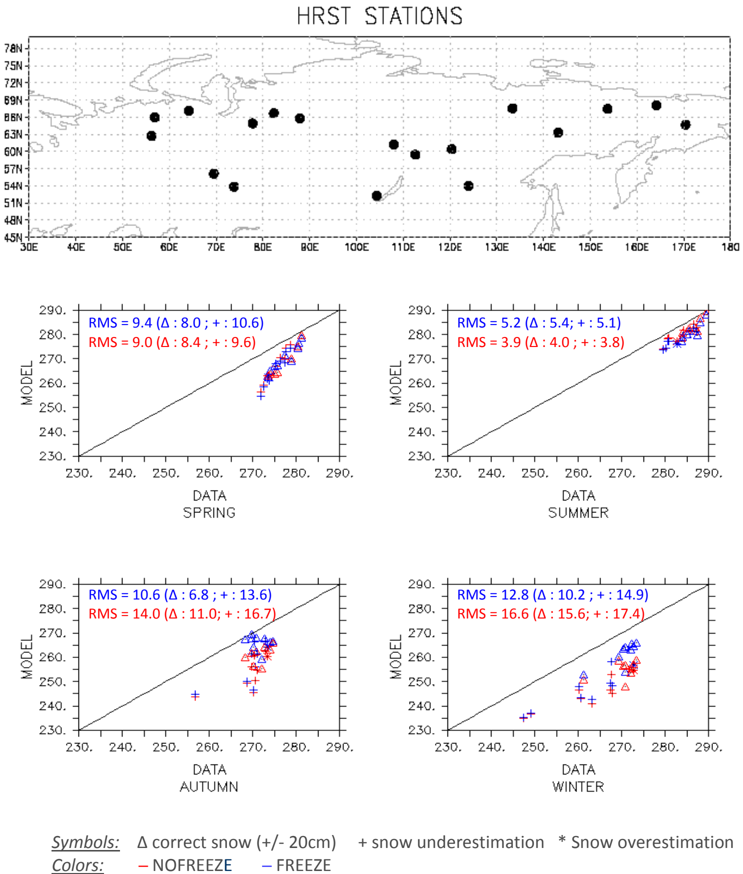

Fig. 8. Top: HRST stations locations. Bottom: comparison between observed (x-axis) and modeled (y-axis) soil temperatures at depths from 0 to 20 cm at the HRST stations for the year 1987. Colors refer to the model with and without the soil new soil freezing scheme; symbols discriminate between the sites where the snow depth is either properly represented by the model within a ±20 cm range (correct snow), or underestimated by the model (snow underestimation) or overestimated by the model (snow underestimation) when compared to the ISLSCP Initiative 1 snow product.

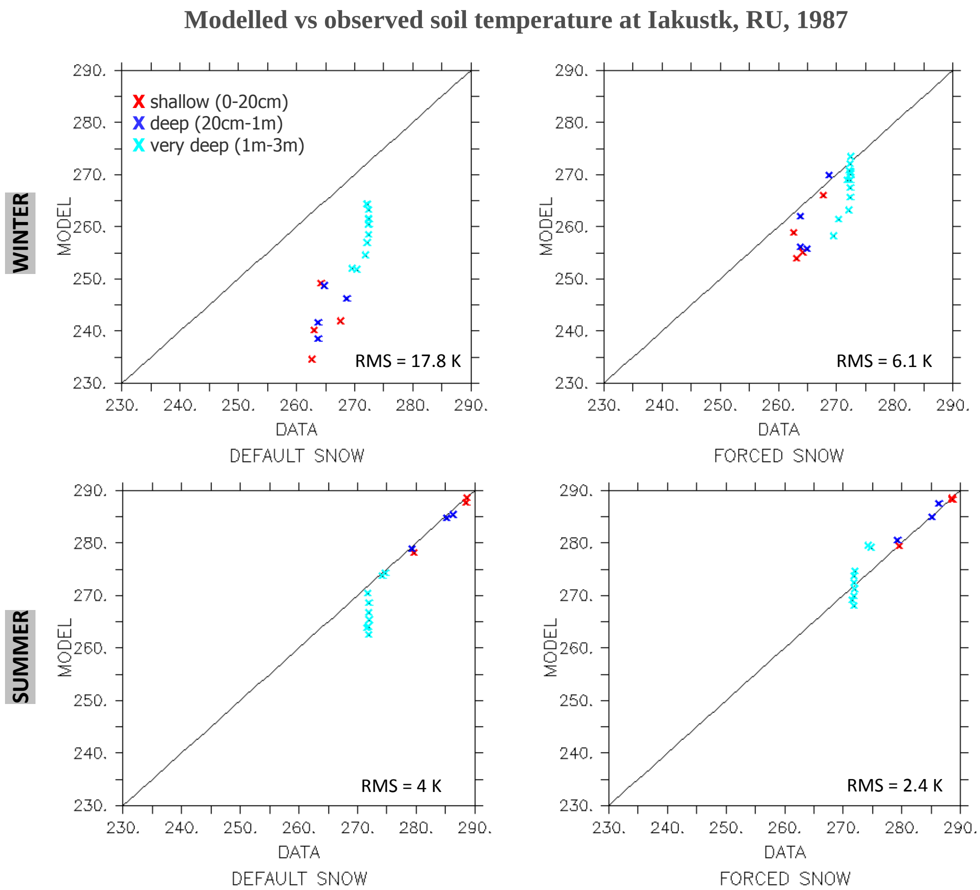

Fig. 9. Comparison between modeled and observed soil temperatures (in K) at different depths (shallow, deep, very deep) at Iakustk in an experiment where the modeled snow depth is underestimated by 30 cm (left) and in the forced-snow experiment (right), where the modeled snow is artificially forced by observations.

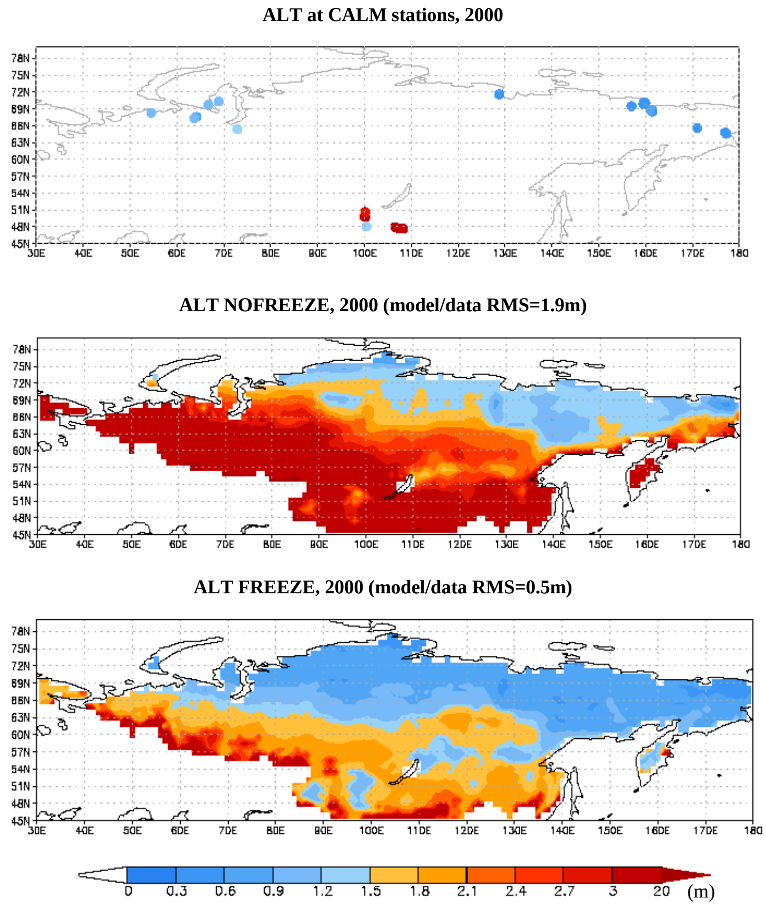

Fig. 10. Active layer thickness (ALT) for the year 2000 as observed at CALM stations (top); as modeled without the soil freezing scheme (center); and as modeled with the soil freezing scheme (bottom).

TCD
5, 2197–2252, 2011

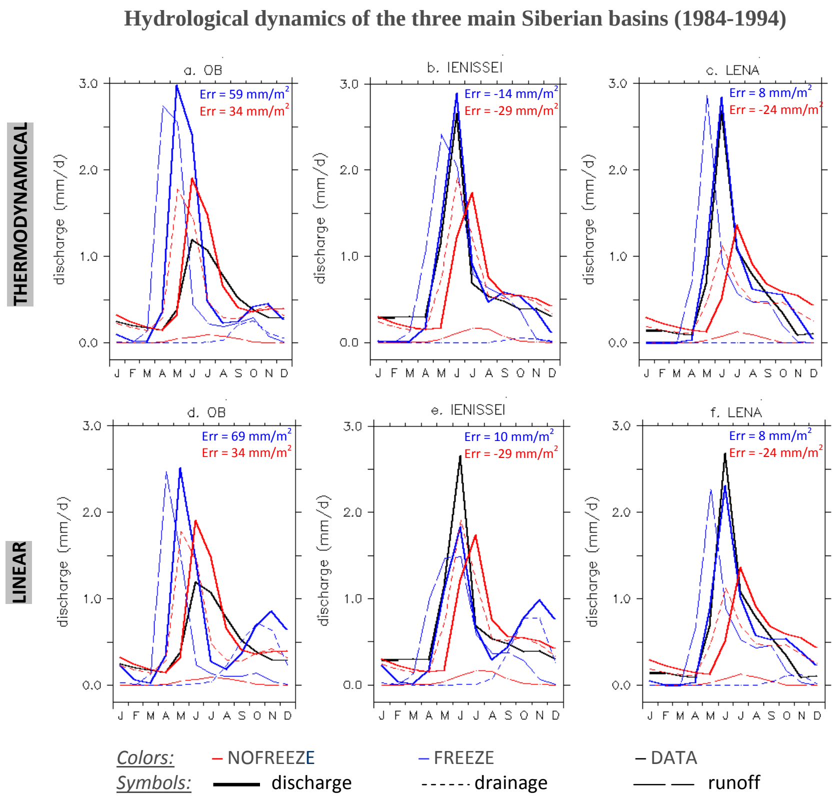

Fig. 11. Mean annual hydrological dynamics of the three main Siberian basins, as simulated with (FREEZE) and without (NOFREEZE) the new soil freezing scheme for the decade 1984–1994, and river discharges from the R-ArcticNET database (DATA). In the upper part the soil freezing scheme uses the thermodynamical parameterization; in the lower part the linear parameterization is used. Plain curves represent the hydrographs at the mouth of the rivers, thin dotted lines the drainage at the bottom of the soil column, and large dotted line the surface runoff. "Err" refers to the mean model error in the cumulated annual discharge over the basins.